Heliyon 9 (2023) e22329

Contents lists available at ScienceDirect

Heliyon

journal homepage: www.cell.com/heliyon

Review article

Zeolitic imidazolate framework as humidity-resistant solid state-chemiresistive gas sensors: A review

Malepe Lesego [a], Derek T. Ndinteh [a], Patrick Ndungu [b], Messai A. Mamo [a,*]

[a] Department of Chemical Sciences, University of Johannesburg, PO Box 17011, Doornfontein, 2028 Johannesburg, South Africa
[b] Department of Chemistry, University of Pretoria, Private Bag X20, Hatfield, 0028, Pretoria, South Africa

A B S T R A C T

With significant technological advances, solid-state gas sensors have been extensively applied to detect toxic gases and volatile organic compounds (VOCs) in confined areas such as indoor environments and industries and to identify gas leakage. Semiconductor metal oxides are the primary sensing materials, although their major drawbacks include a lack of sensitivity, poor performance at high humidity, and operating at high temperatures ranging between 140 and 400 °C. Recently, the use of zeolitic imidazolate frameworks (ZIFs) in gas sensors has received considerable attention as a promising material to overcome the drawbacks possessed by semiconductor metal oxide-based gas sensors. Because of their unique properties, including size tunability, high surface area, and stability in humidity, ZIF becomes a preferred candidate for sensing materials. The use of ZIF materials in gas sensors is limited because of their high-temperature operation and low gas responses. This review outlines the strategies and developments in the utilization of ZIF-based materials in gas sensing. The significant influence of the addition of carbon additives in ZIF materials for temperature operation sensors is discussed. Finally, ZIF-carbon additives and SMO@ZIFs/carbon additives are the proposed materials to be studied for future prospects for the detection of VOCs at low temperatures and exhibiting good selectivity towards the gas of interest.

1. Introduction

Air pollution can be defined as the presence of released harmful volatile chemicals in the atmosphere that harm the health of humans and animals and the balance of land and sea ecosystems. Major sources of air pollution include industrial factories, mineral dust, and agricultural burning [1]. The health of living organisms can be maintained by ambient air monitoring of gases released by industrial companies such as the coal, electricity, and mining industries. In 2013, the EU Environmental Protection Agency reported that 46 700 people died from air pollution, labelled "the largest environmental hazard," while the UK reported 40 000 deaths [2].

Death-leading toxic gases include hydrogen sulfide (H_2S) [3], carbon dioxide (CO_2), sulfur dioxide (SO_2) [4], and nitrogen dioxide (NO_2) [5]. Volatile organic compounds (VOCs), such as methanol, ethanol [6], formaldehyde, acetone, and toluene [7], are primarily utilized in paints, cosmetics, detergents, dyes, drugs, and plastics. Severe inhalation of VOCs vapour is dangerous to human health because it can cause bronchitis, eye inflammation, and dizziness [8,9]. Flammable gases such as H_2 and CH_4 cause unexpected explosions or fires [10]. This has led researchers and engineers to develop friendly hazardous gas-detecting devices for environmental monitoring. Gas sensors are required to ensure good air quality and reduce explosions caused by flammable gases.

The critical quality control for good health and safety in industrial emissions is the online detection and identification of emitted toxic, flammable gases and volatile organic compounds. High concentrations of inhaled poisonous gases and volatile organic compounds (VOCs) can cause new deaths in hospitalized patients.

Reports have shown that air quality can be monitored using cost-effective gas-sensing devices. Therefore, solid-state gas sensors

* Corresponding author.
E-mail address: messaim@uj.ac.za (M.A. Mamo).

https://doi.org/10.1016/j.heliyon.2023.e22329
Received 7 June 2023; Received in revised form 16 October 2023; Accepted 9 November 2023
Available online 15 November 2023

received significant attention because of their low cost production, excellent selectivity, and effective detection [2]. Therefore, finding a cost-effective, highly sensitive, and selective gas sensor for environmental air monitoring and disease detection remains a priority in the field of research. Some requirements of these devices include portability, and the sensor needs to be cost-effective and do online or in-situ gas sensing to monitor the leakage of gases produced in large buildings and industrial applications. The major challenges in gas sensors are to improve sensitivity and selectivity towards the gas of interest, have a quick response and recovery time, operate at lower temperatures, have a sensor with a good lifespan, and be resistant to humidity fluctuations. In the past, semiconductor metal oxides (SMOs) have been the most studied and promising materials for detecting and monitoring toxic gases; however, they possess some significant drawbacks that make the sensor fail to be applied in real applications, such as high-temperature operation and a lack of selectivity [7]. Several methods, such as doping SMOs with noble metals and designing SMOs-SMOs hybrids, were used to improve the sensing performances, such as sensitivity and response-recovery times; however, their high operating temperatures make it difficult for real-life applications [8].

Furthermore, the successfully prepared carbon additives-SMOs hybrids were able to drop the high operating temperature to room temperature sensing; sensors are affected by the change in humidity, and selectivity still needs improvement. Thus, the utilization of the zeolitic imidazolate frameworks with carbon additives are promising candidates to operate at room temperature, have good selectivity, and be resistant to changes in humidity because the tunability of ZIFs pore sizes can improve selectivity and also be hydrophobic [9,10]. The following sections discuss the development and significance of ZIFs in SMOs and carbon additives; their sensing properties are also discussed.

2. Chemiresistive gas sensor

2.1. Introduction to sensor

Sensors measure or monitor the physicochemical changes in the environment [11]. Three main classes of sensors are classified according to the properties the device is sensing: physical sensors [12], biosensors [13], and chemical sensors [14]. Physical sensors reveal information about physical parameters such as temperature, mass change, pressure, or moisture in the environment. A biosensor is a sensor designed to detect and measure substances by combining the analyte with a specific biological recognition, such as enzymes, proteins, or nucleic acids [15]. Chemical sensors reveal chemical interactions between the device and the analyte.

A typical gas sensor mainly consists of a sensing material and a transducer. The sensing material chemically interacts with the gas of interest. Subsequently, it captures the changes in the sensing material's electrical, optical, and magnetic properties into readable data that can be displayed on the monitor. For example, the sensor's electrical properties change during the interaction between the gas analyte and sensing material, as measured by the transducer [14]. Solid-state gas sensors are in demand because of their easy operation, low cost, and innovations in line with advancing technology. Solid-state sensors are designed such that there is no mobile component, such as an electrolyte [11,14,15].

2.2. Chemiresistive gas sensors

Chemiresistive sensors are the type of gas sensors that are mostly studied and applied in commissioning because of their cost-effectiveness, simplicity of fabrication, ease of use, and portability. There is considerable interest in improving chemiresistive gas sensors owing to their major challenges, including high-temperature operation, selectivity towards the gas of interest, and long-term stability. Chemiresistor gas sensors mainly comprise two terminal electrodes connected to a sensing layer, typically a semiconductor metal oxide. During the interaction of the analyte gas with the thin film of the sensing materials, the current flow changes, which causes changes in the resistance of the sensors [16].

3. Performance evaluation of gas sensors

Gas sensor performance was examined by analyzing the response time, recovery time, sensitivity, limit of detection (LOD), precision, selectivity, stability, life cycle, working temperature, and fabrication costs [17]. The sensitivity is determined by the ratio Ra/Rg for the gas of interest, where Ra is the gas sensor resistance in the air (known as a reference gas), and Rg is the resistance of the gas sensor to the gas analyte. The sensitivity can also be expressed as $[(Ra-Rg)/Ra] \times 100\ \%$ [18,19].

Selectivity is a method by which a sensor can identify and detect the gas of interest in a mixture of gases. Precision is a measure by which a gas sensor can reproduce similar results and is also known as repeatability. LOD measures the lowest gas analyte concentration that a gas sensor can detect. The response time is when the sensor produces a signal corresponding to a specific gas concentration. Recovery time is the time the sensor takes for the corresponding signal of the gas to return to its initial value after a step concentration change [18].

Stability is a way in which a sensor can reproduce results for a long time. In terms of stability, an ideal gas sensor should operate for approximately 2–3 years, which is almost equivalent to 17 000–26 000 h of operation. It is prefered for gas sensors to operate at lower temperatures and have lower fabrication costs. The performance of different materials (carbon materials, polymers, catalytic metals, and SMOs) used in gas sensors was evaluated using the abovementioned parameters [18,19].

4. The surface chemistry of the sensors

4.1. General sensing mechanism

Basic semiconductor metal-oxide (SMO) sensing processes explain the general sensing mechanism. SMO gas detection relies on the availability of acceptor oxygen molecules absorbed on the active layer's surface via an ionosorption process. The absorbed oxygen molecules accept electrons from the active sensing layer to form ionized reactive oxygen species (ROS), including O_2^-, O^-, and O^{2-}, depending on the working temperature of the active sensing material. Gas sensors that work below 100 °C use oxygen ions (O_2^-), and temperatures between 100 and 300 °C convert O_2^- into O^- as it captures some electrons, while temperatures above 300 °C convert O^- ions into O^{2-}. Summarized formulae for forming reactive species in the active layer [20,21].

$$O_{2\ (gas)} \leftrightarrow O_{2\ (ads)} \tag{1}$$

$$O_{2\ (ads)} + e^- \leftrightarrow O_{2\ (ads)}^- \text{ below } 100\ ^\circ C \tag{2}$$

$$O_{2\ (ads)}^- + e- \leftrightarrow 2O^-\ (ads)\ 100–300\ ^\circ C \tag{3}$$

$$O^-_{\ (abs)} + e- \leftrightarrow O^{2-}_{\ (abs)} \text{ above } 300\ ^\circ C \tag{4}$$

The adsorbed oxygen molecules accept electrons from the SMO active sensing layer, and the electrons tend to become trapped on the surface as ions, leading to band bending. As oxygen accepts electrons from the working material, it depletes them. As illustrated in Fig. 1, active reactive oxygen species interact with the gas of interest, which can either be reducing or oxidizing agents, forming water vapour and carbon dioxide.

The majority of carriers in n-type SMO are electrons; hence, the absorbed oxygen ions accept electrons from the conduction band of SMO. The conductivity of the active layer of SMO decreases as electrons are trapped on the surface by the absorbed oxygen molecules; hence, the resistance increases. Depending on the type of analyte gas (reducing or oxidizing), conductivity increases or decreases when the absorbed oxygen ions interact with the gases. The carriers in p-type SMO are holes; there is a decrease in resistance or an increase in conductivity when absorbed oxygen ions interact with oxidizing gases [22], and the opposite is true for reducing gases.

4.2. Band bending

When a sensor is supplied with a DC or AC voltage, the electrons passing through the material grains are trapped by oxygen molecules that are absorbed on the surface, leading to band bending [21,23]. Band bending occurs during the interaction of the exposed donor gas analyte with the SMO on the sensing element, wherein the conduction band loses electrons through the extraction process onto the surface, leading to an electron depletion layer. Since the electrons on the depletion layer are negatively charged, it leads to band bending, which generates a potential barrier at the surface (see Fig. 2). There is a reverse band bending, which results in the reduction of potential barriers during the desorption of absorbed oxygen ions and reducing gases on the surface.

4.3. Semiconductor metal oxides in gas sensors

The use of nanomaterials over conventional bulk-scale materials in device fabrication has increased exponentially in the past decade as they have improved many devices, such as solar cells [24], sensors, batteries [25], and supercapacitors [26]. The unique properties displayed by nanomaterials include a high surface-to-volume ratio and good electrical properties. Still, a significant achievement is the detection and monitoring of traces of targeted analytes such as gases, heavy metals, and biomolecules in various applications [24–26]. Semiconductor metal oxides (SMOs) such as SnO_2 [27], ZnO [28], TiO_2 [29,30], NiO [31,32], and MnO_2 [33–36] are the most promising materials for the fabrication of gas sensors; however, they operate at high temperatures of 140–400 °C. The subjection of the devices to high temperature results in material degradation, which causes a shorter lifespan for the devices [37].

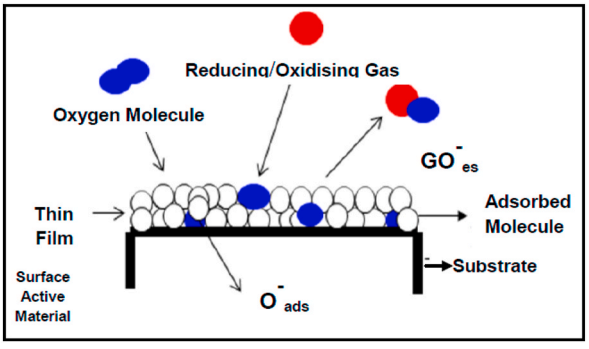

Fig. 1. Schematic representation of the active sensing layer interacting with the gas of interest [7].

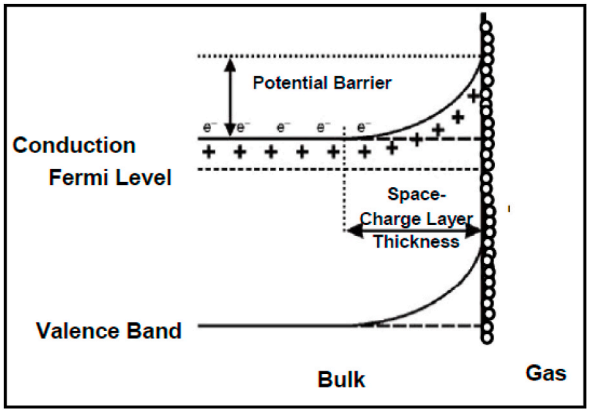

Fig. 2. Schematic of band bending during gas sensing of N-type SMO [21].

In SMO gas sensors, it is difficult to control the sensor to detect the targeted gas only, and it also consumes a lot of energy for their operation, which are two significant drawbacks of utilizing SMOs in gas sensors [33,35,36].

5. Zeolitic imidazole framework

Due to their unique properties, metal-organic frameworks (MOFs) are currently used in gas-sensing applications. The drawbacks of high-performing inorganic SMOs are improved by introducing organic functionalities, modifying the metal oxides with gas filtering materials for specific gases, and using core-shell materials [37]. Recently, gas sensors with higher selectivity have been developed using gas-filtering porous polymers and metal-organic framework (MOF) composites. MOFs are materials consisting of organic ligand molecules on metal ions [38]. There is great interest in improving the selectivity, and sensitivity of gas sensors by coating metal oxide nanowires or nanorods with zeolitic imidazole frameworks (ZIFs) [39]. ZIFs are a subclass of MOFs with a zeolite structure known as a tetrahedral network, wherein the organic linker is imidazolate [39,40].

The imidazolate linkers were coordinated to a transition metal, Zn, Fe, Cu, or Co. There are several tetrahedral frameworks containing imidazolate linkers, including ZIF-7 [41], ZIF-9 [42], ZIF-8 [38], ZIF-11 [43], ZIF-67 [9], ZIF-68, and ZIF-71 [44]. Some of the ZIFs crystal structures are shown in Fig. 3. Highly crystalline materials are chemically robust, thermally stable, and porous. ZIFs are considered promising materials for gas sensing devices owing to their tunability in pores and functionality, improving gas selectivity and operating at room temperature. The most commonly applied metal oxide gas sensors exhibit humidity interferences; however, in the past, ZIF-8 and ZIF-71-based gas sensors have been reported to inhibit humidity interactions due to the hydrophobicity of the material [44].

ZIF-7 is the earliest reported tetrahedral framework of benzo-imidazole ligands coordinated to divalent zinc cations through a nitrogen donor. All ZIFs are formed through a dative bond between the N-imidazole and a metal cation. ZIF-8 is a tetrahedral zeolitic framework containing a 2-methyl imidazolate linker coordinated to a divalent zinc cation [37], while in ZIF-71, the Zn^{2+} is linked through the 4,5-dichromoimidazilate linkers. Tetrahedral arrangements form spheres or pores within the framework responsible for gas storage, separation, and sensing [46]. ZIF and SMOs composites are stable and have higher selectivity and sensitivity towards the gases of interest. SMO-ZIF-based sensors block moisture sensing interference during gas detection, a major challenge for SMOs gas sensors [47].

6. Methods of synthesis, morphology, and thermal analysis

These highly ordered, intrinsically mesoporous, and microporous materials can be prepared using different synthetic approaches. Nanostructured ZIFs were synthesized by controlling the synthetic parameters, including the temperature, reaction time, amount of surfactant added, and concentrations of the reactants. The reaction time controls the pore diameters and sizes of the ZIF particles. The most popular methods for the synthesis of sol-gel are hydrothermal and solvothermal. Complementary methods for synthesizing ZIFs include microwave and mechanochemical synthesis [48,49].

6.1. Synthesis of ZIF-8

ZIF-8 particles of four different sizes were synthesized under controlled conditions. Size-controlled ZIF-8 can be synthesized at room temperature by dissolving a calculated amount of zinc nitrate hexahydrate and 2-methylimidazole in methanol. A specific amount of sodium formate follows this to get the respective sizes. All the SEM images of ZIF-8 showed a rhombic structure (Fig. 4). The synthesis temperature and amount of sodium formate were directly proportional to the particle size of ZIF-8 [50].

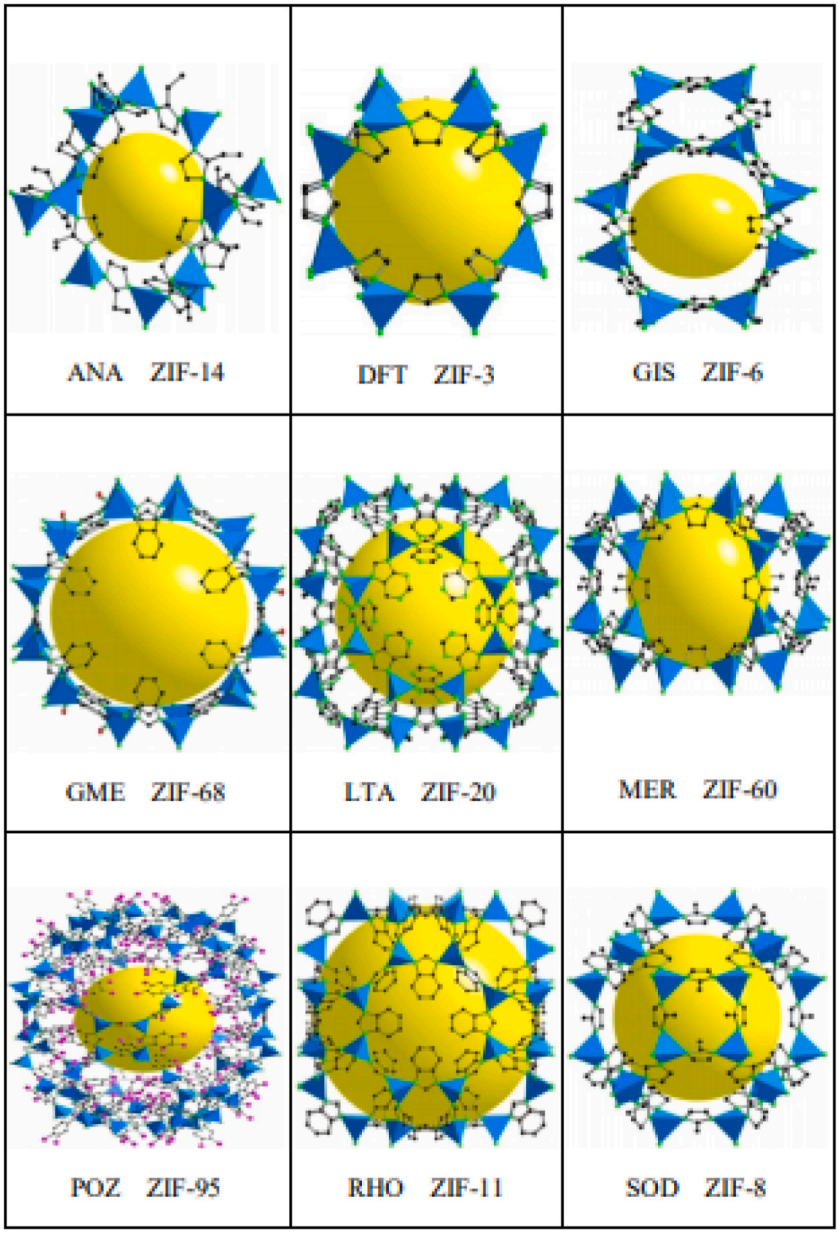

Fig. 3. Different crystal structures of ZIFs [45].

6.2. Synthesis of ZIF-67

ZIF-67 can be synthesized in various particle sizes depending on the reagents used and the applied reaction conditions [see Fig. 5]. Bulk ZIF-67 can be synthesized using a solvothermal method using cobalt acetate tetrahydrate and 2-methylimidazole. Next, cobalt nitrate hexahydrate and 2-methylimidazole were used to synthesize ZIF-67. Fig. 6 clearly shows that the synthesis of ZIF-67 at higher temperatures resulted in particle growth via aggregation. The synthesis temperature is directly proportional to the particle size. Transmission electron microscopy (TEM) revealed that the ZIF-67 structures were rhombic dodecahedral [52] (see Fig. 7).

6.3. Synthesis of ZIF-7, ZIF-65-Zn and ZIF-71

ZIF-7 was assembled by coordinating Zn^{2+} with the benzimidazole ligand, while Z1F-65-Zn was synthesized by linking Zn^{2+} with 2-nitroimidazole. ZIF-71 was formed by linking the Zn^{2+} ion to a 4,5-dichloroimidazole. It has been reported that the synthesis of nano ZIF-7 and ZIF-71 requires approximately 48 h, with a lower yield of roughly 12 %. Typically, ZIF-71 is synthesized by weighing a

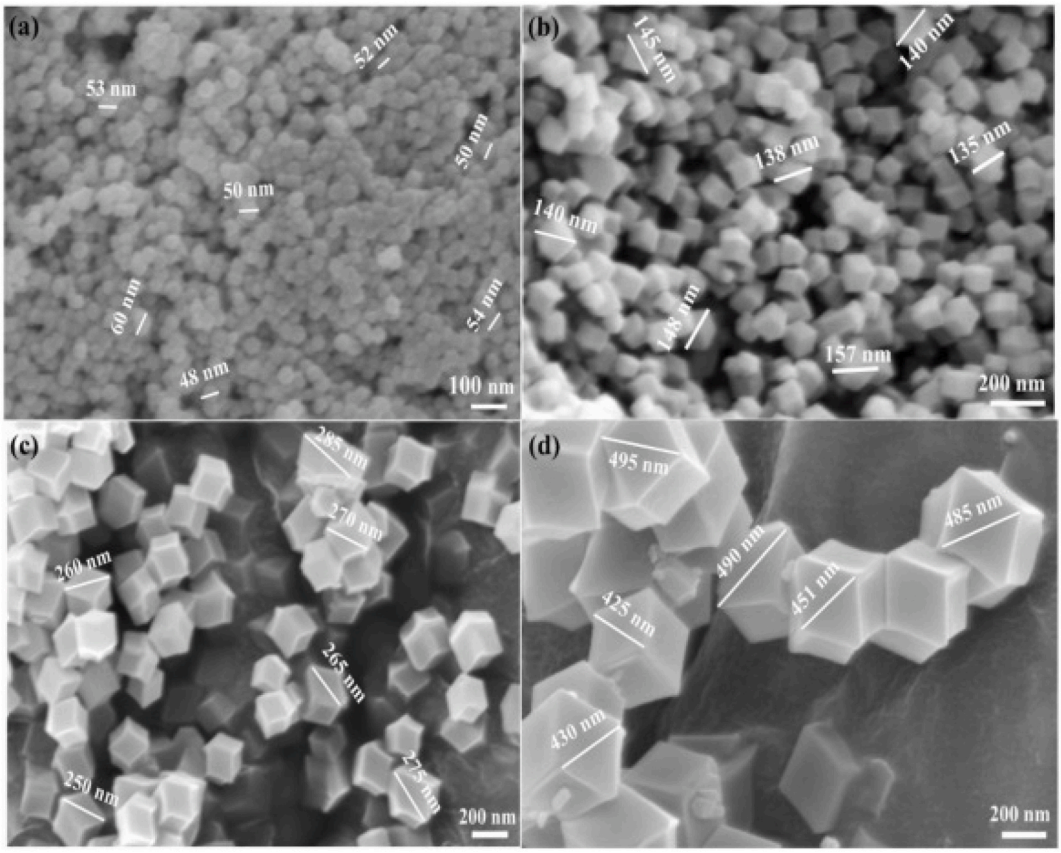

Fig. 4. SEM images of ZIF-8 at (a) 60 nm, (d) 140 nm, (c) 260 nm, and (d) 480 nm [51].

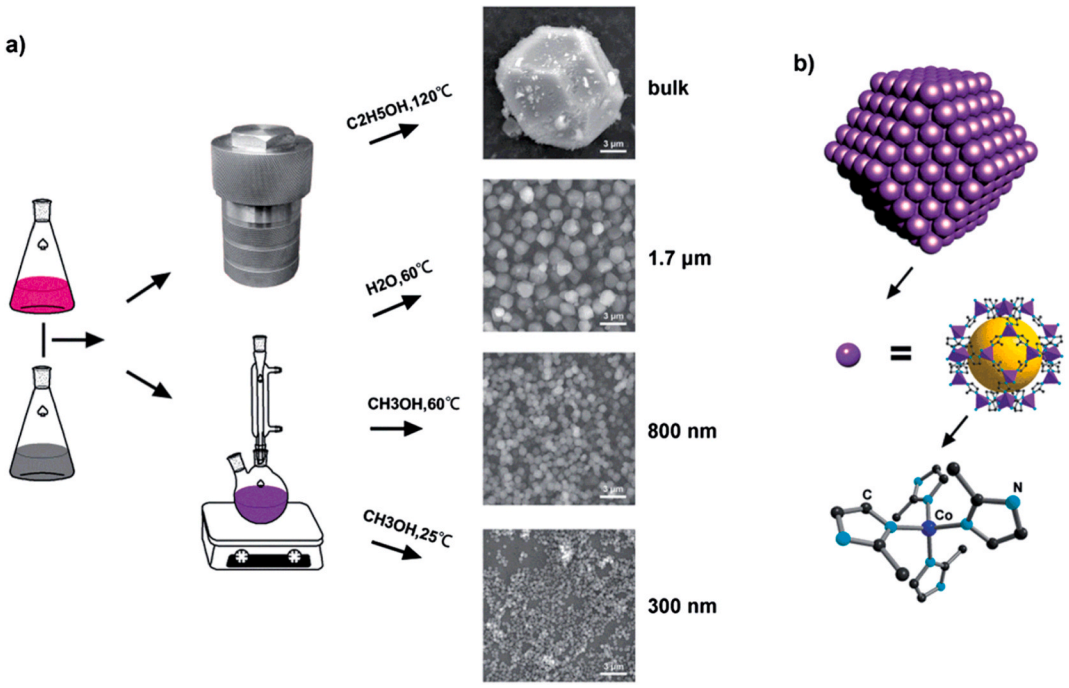

Fig. 5. Schematic illustration showing the synthesis of ZIF-67 using various particle sizes [52].

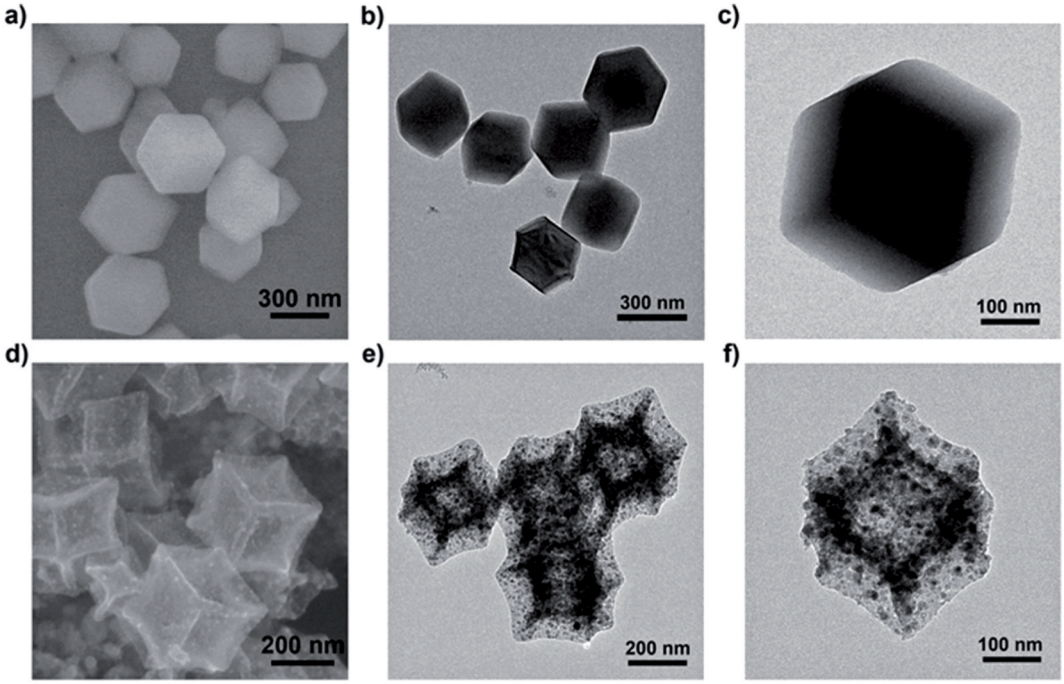

Fig. 6. TEM images of 300 nm prepared ZIF-67 [52].

powder sample of 110 mg zinc acetate dihydrate (0.5 mmol) and 160 mg 4,5-dichloroimidazole (1 mmol) in 5 mL of DMF and 5 mL of methanol, respectively. The zinc solution was transferred to a 4,5-dichloroimidazole linker solution, immediately after which the solution turned milky and the reaction was continuously stirred for 30 min. Precipitates were formed and filtered through centrifugation by washing three times with methanol [53]. The TEM images of ZIF-7, ZIF-65-Zn, and ZIF-71 present cubic-like structures with an average diameter of 100 nm, 120 nm, and 90 nm, respectively.

6.4. Decoration of SMOs with ZIFs

Nanomaterials play a crucial role in gas sensing applications because they can be synthesized in various morphologies, including nanorods, nanoflowers, and nanowires. They exhibit higher surface areas and reactivities, which enhance the sensing performance [37,54,55]. Zero-dimensional (0D) nanospheres or nanoparticles usually have a high surface area but can easily agglomerate, decreasing gas-sensing performance as the number of active sites becomes narrower [56]. However, the use of one-dimensional (1D) nanotubes [51,57], nanorods [58], and nanowires [59–61] of SMOs received significant attention for gas sensing applications because of their higher surface area and higher porosity. 1D nanostructured SMOs have more positive attributes in gas-sensing applications than 0D nanostructured SMOs. Thus, ZIFs are currently prepared through the decoration or encapsulation of nanorods [62] and nanowires [63] with imidazolate ligands, as shown in Fig. 8. For the preparation of ZIF through the encapsulation of SMOs, the 1D nanostructured SMOs are primarily prepared through a hydrothermal synthetic method. This was followed by solvothermal treatment, wherein the prepared 1D nanostructured metal oxide was mixed with the imidazolate linker of interest, depending on the desired output, in a mixture of two solvents, dimethylformamide (DMF) and water, at a 3:1 ratio. The 1D nanostructured SMOs act as a structural template for the ZIFs, whereas the ZIFs retain the 1D nanostructured structure, as shown in Fig. 8 (a) and **(b)** [37].

6.5. The effect of parameters on ZIF-based synthesis

The choice of solvent in ZIF synthesis is critical because ZIFs do not form in water or just any solvents. And among all the investigated solvents, alcohols (especially methanol) and DMF were suitable for ZIFs. The type of solvent chosen, temperature, time, and pH lead to the desired morphology, particle size, and surface area, which play a crucial role in sensing [64]. For instance, a higher surface area results in a high rate of gas molecule adsorption, which enhances gas response during sensing. Different types of morphology result in different sensing performances; thus, the synthesis of ZIFs is very important [65].

6.6. The effect of thermal, chemical, and pore sizes properties in sensing

Thermogravimetric (TGA) analysis is used to determine the thermal decomposition of materials. Fig. 9 (a) and (b) present TGA profiles that revealed that ZIF-8 and ZIF-9 lose approximately 17 % weight percentage at the temperature of 180 °C for the elimination

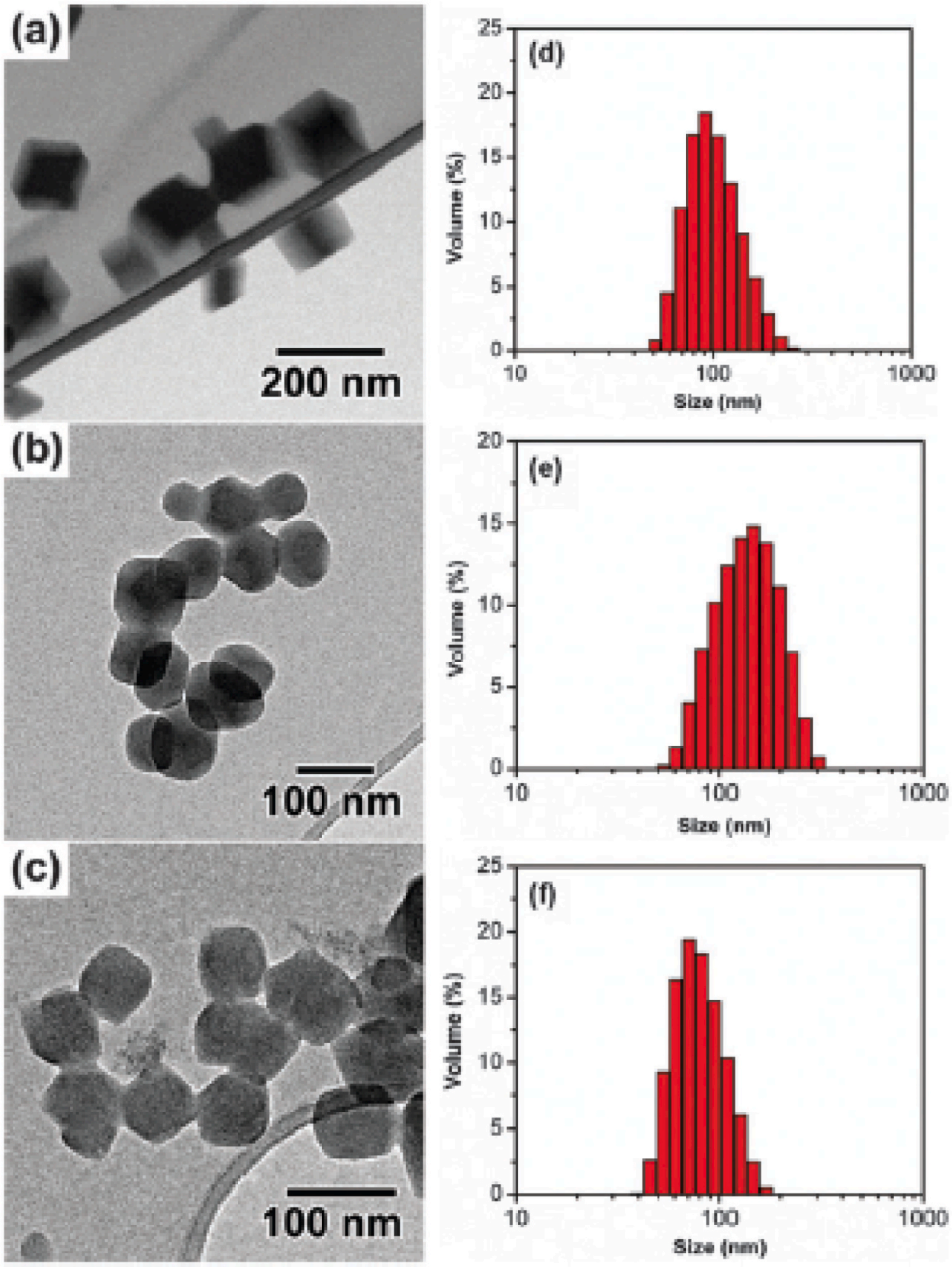

Fig. 7. TEM images of (a) ZIF-7, (b) ZIF-65-Zn, and (c) ZIF-71 and their respective particle sizes [53].

of NH_4^+, and become stable until 450 °C, which is equivalent to the decomposition temperature of ZnO [66,67]. The TGA profiles of ZIF-71 and ZIF-67 are the same (see Fig. 9 (b) and (d)); the materials are stable until they degrade at 450 °C. Some ZIF-based materials are filled with NH_4^+ in the pores. But generally, ZIF materials are thermally stable until 450 °C [68,69]. In addition, SMOs gas sensors operate at a temperature between 150 and 400 °C; thus, introducing ZIFs into SMOs does not limit the optimization of the gas sensors as they can be tested in a wide range of temperatures. Moreover, the thermal stability of the materials is not important enough to be investigated for sensors that operate at room temperature (about 23–25 °C).

A work reported by K. S. Park *et. al*, proved that ZIF materials are stable in many solvents. ZIFs, including ZIF-8 and ZIF-11, were soaked in various solvents such as benzene, water, methanol, and sodium hydroxide separately at their boiling temperatures (80 °C, 100 °C, 65 °C, and 100 °C, respectively) for a week. Periodically, the process was examined and studied under a microscope to study decomposition or the formation of new structures; fortunately, the immersed ZIFs were found to be stable in various chemical

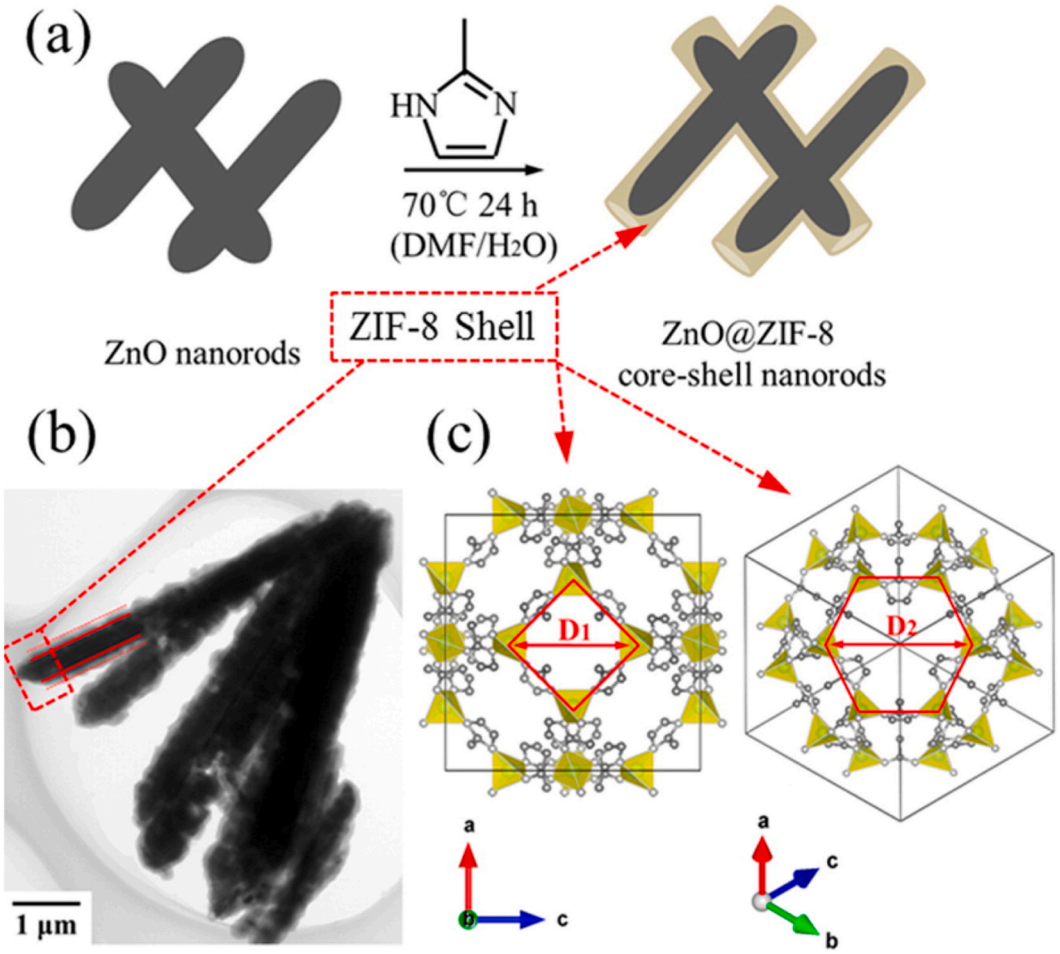

Fig. 8. (a) ZnO nanorods and ZnO@ZIF-8 core-shell nanorods, (b) TEM image of ZnO@ZIF-8, and (c) tetrahedral map of ZnO@ZIF-8 [37].

conditions [70]. This factor is advantageous to gas sensing since the analytes cannot be permanently attached or bonded to ZIF-based materials since most gas sensors use an adsorption-desorption sensing mechanism.

ZIFs are unique materials with different pore sizes, and the pore sizes of ZIFs are controllable during synthesis, which can work as an advantage to control the selectivity to a gas of interest. The pore diameters of ZIF-8, ZIF-11, ZIF-67, and ZIF-71 are 11.6 Å, 14.6 Å [5], 0.32 nm [71], and 4.8 Å [71], respectively. Gases and molecules have their specific kinetic diameters; for example, the kinetic diameters of ethanol, benzene, acetone, and hydrogen range between 2.89 Å and 5.85 Å [72]. Consequently, if the kinetic diameter of the molecules is smaller than the pore size diameter of the materials, then there is a high probability that the sensor will have poor selectivity because all the analytes pass through and get detected. In addition, if the material has a smaller pore size diameter than the kinetic diameter of the vapour analyte, then there is a high probability that there will be no sensing or show small gas responses [73]. ZIFs materials repel water molecules, which is advantageous as the gas sensors are water vapour resistant [9]. With all the advantages mentioned above, ZIFs are more promising candidates to be utilized in gas sensing than pristine semiconductor metal oxides. The selectivity of the targeted gas can also be determined by the chemical interaction between the ZIF-ligands and the organic functionality of the analyte [73,74].

7. ZIF- based sensor strategies and design

7.1. Bi- ZIF gas sensors

In recent years, gas sensors have been developed by combining nanostructured SMOs with carbon-based materials and conducting polymers. However, the pristine ZIFs (as a single material) performed well in gas sensing due to their unique tetrahedral structure, higher surface area, and size-exclusion nature, with improved selectivity for the gas of interest. Recently, combining two different ZIFs exhibited excellent results compared to ZIF as a single material [66]. Bi-ZIF gas sensors are gas sensors fabricated from the combination of two different ZIFs; the composite can be obtained by combining any two ZIFs from ZIF-7, ZIF-8, ZIF-9, ZIF-11, ZIF-65, and ZIF-68,

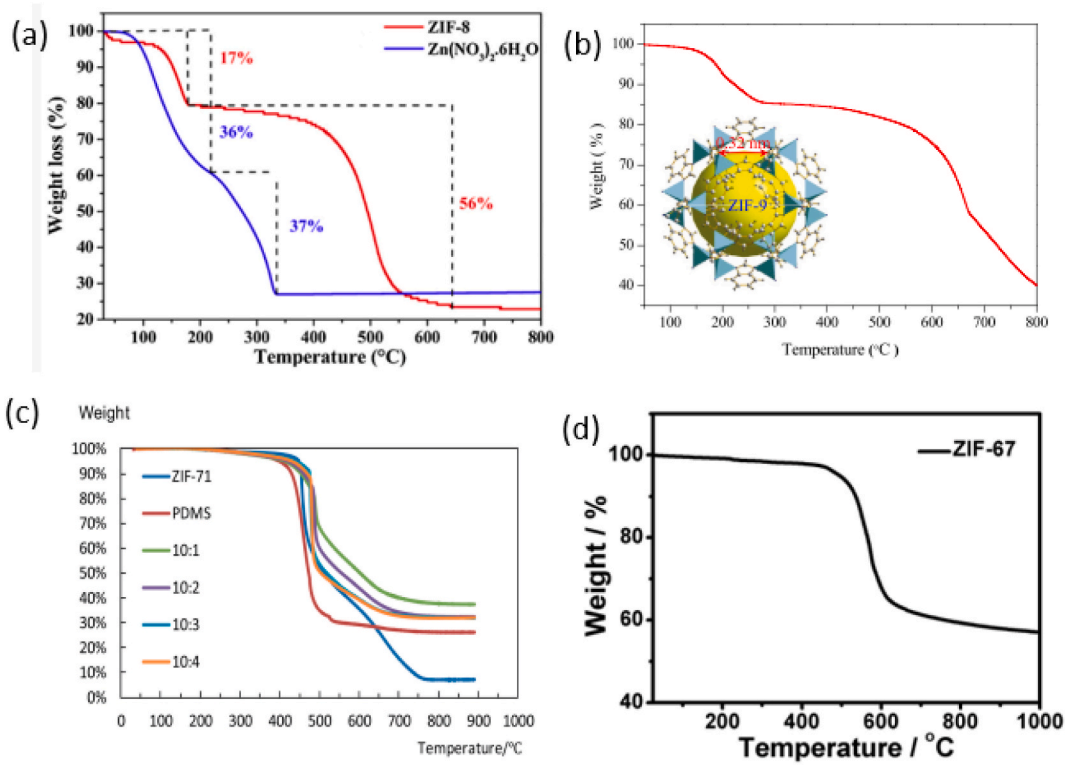

Fig. 9. TGA profiles of (a) ZIF-8, (b) ZIF-9, (c) ZIF-71, (d) ZIF-67.

ZIF-67, ZIF-71, ZIF-90 and more. Fig. 10 shows ZIF-67 and ZIF-8+ZIF-67 chemiresistive sensors for detecting hydrogen gas at 180 °C, wherein combined ZIF-8 and ZIF-67 showed a 5.1 times higher response than the ZIF-67 sensor alone [75]. Fig. 10 (b) shows the response relativity of toluene, ethanol, hydrogen, carbon monoxide, and nitrogen dioxide at different concentrations of 10, 25, 50, 75, and 90 ppm, where all combined ZIF-8 and ZIF-67 sensors showed higher responses than the ZIF-67 sensor. Finally, it was clearly shown that ZIF alone and its combination derivatives could detect gases using a solid-state gas sensor and have good repeatability, selectivity, and fast sensing responses. The working temperatures of these sensors are incredibly high, and there are high ignition risks during the detection of highly flammable gases (hydrogen gas).

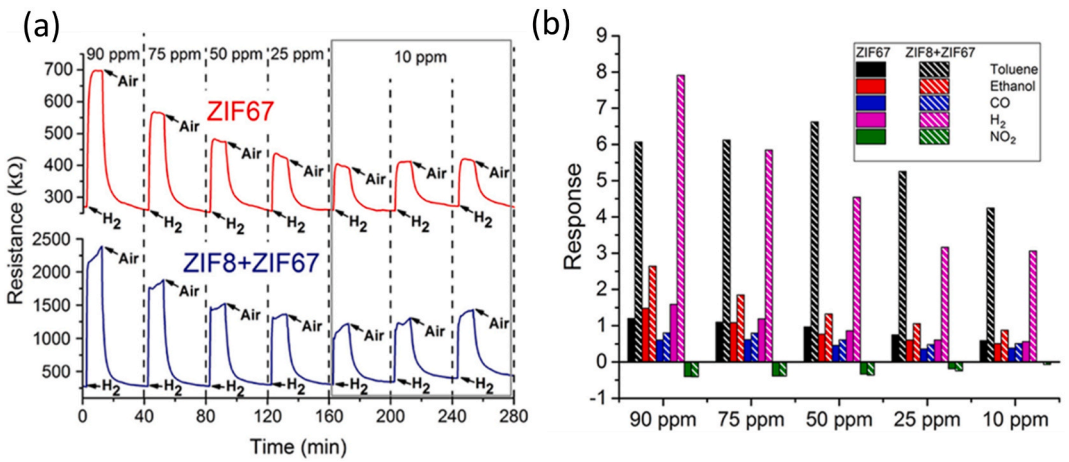

Fig. 10. (a) Real-time chemiresistive hydrogen gas sensing at different concentrations and (b) relative responses of different analytes at different concentrations for ZIF-67 and ZIF-8+ZIF-67 sensors [75].

7.2. SMOs@ZIFs composite sensors

The combination of nanostructured ZIFs and SMOs showed improved gas-sensing performance compared to individual materials such as SMOs and ZIFs sensors. Although solid-state chemiresistive gas sensors have been reported to be effective in sensing applications, ZnO@ZIF-8 has better sensitivity for detecting formaldehyde than ZnO nanorods, as shown in Fig. 11 (a-d). ZnO@ZIF-8 sensor is four times more formaldehyde sensitive than ethanol, ammonia, acetone, methanol, and toluene vapours. The introduction of ZIF-8 improved sensitivity because of its unique size-exclusion nature, wherein formaldehyde has a kinetic diameter of 2.43 Å and while 2.90 Å, 3.60 Å, 4.43 Å, 5.25 Å are the kinetic diameters of ammonia, methanol, ethanol, acetone, and toluene, respectively. ZIF-8 allows only formaldehyde to pass through the pores easily other than all mentioned VOCs because ZIF-8 has a pore size aperture of 3.40 Å. Ammonia has a low response on the ZnO@ZIF-8 sensor. However, it has a small kinetic diameter to pass through ZIF-8 easily because the ZnO sensor blocks the ammonia response, as shown in Fig. 11 (b). The ZnO sensor has a higher response to formaldehyde than the ZnO@ZIF-8 sensor at the optimal temperature of 300 °C; however, the ZnO@ZIF-8-based sensor is preferred over the others because it has higher selectivity than the ZnO sensor and works even with humidity interference [37].

In addition to the use of sensors under humid conditions, bimetallic ZIF-based materials, such as ZIF-67 (Co) and ZIF-8 (Zn) with ZnO, have been used to fabricate ZnO@ZIF-CoZn sensors. The ZnO@ZIF-CoZn-based sensor showed 20 times higher response and a

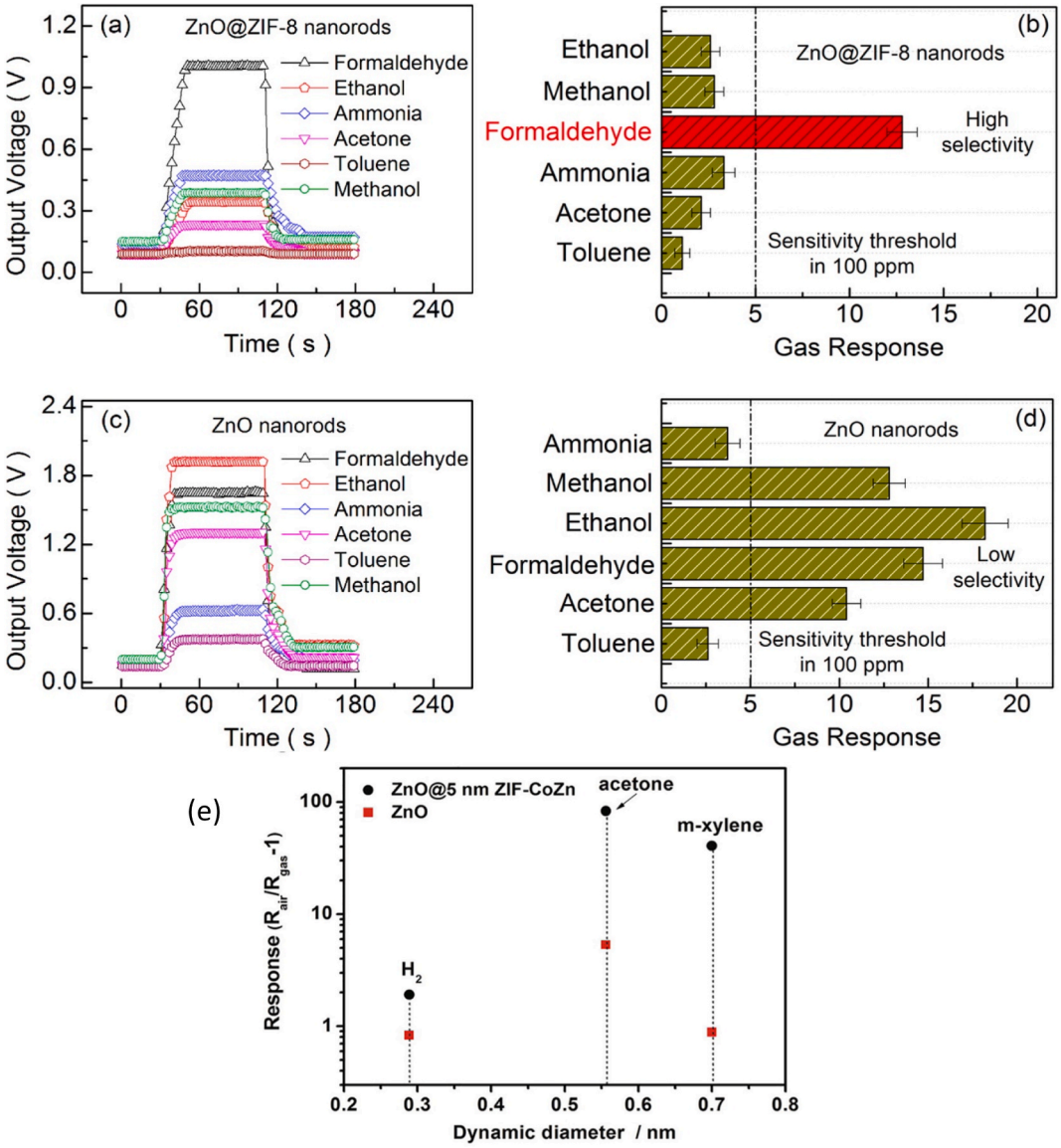

Fig. 11. (a,b) Gas response and selectivity graph of ZnO@ZIF-8 for different analytes, (c,d) gas response and selectivity graph of ZnO sensor for different analytes and gas responses of ZnO [43], and (e) ZnO and ZnO@ZIF-CoZn sensors to different analytes (100 ppm) at 260 °C [54].

100 times improved LOD than the ZnO-based sensor, as shown in Fig. 11 (e), and the working temperature of the sensor was reduced by over 120 °C from 385 to 260 °C. The ZnO@ZIF-CoZn sensor responded to gaseous analytes, such as hydrogen, acetone, and m-xylene; however, the highest sensitivity for acetone was recorded. The kinetic diameter of ZnO@ZIF-CoZn is 5 nm, while the analytes have a kinetic diameter of 0.3, 0.51, and 0.7 nm for hydrogen, acetone, and m-xylene, respectively. In this case, ZnO played a significant role by being more responsive to acetone than to hydrogen and m-xylene, and the ZIF-ZnCoZn only improved the sensitivity of the ZnO sensor [54]. The kinetic diameter of ZnO@ZIF-CoZn did not significantly improve the selectivity towards the gas of interest because all analytes could penetrate the pore spaces of the material. One way to enhance the selectivity of these analytes is to reduce the dynamic diameter of the sensing material.

7.3. Metal doping on SMOs@ZIF composite sensors

In addition, the effect of doping on ZIF and SMOs composite sensors plays a crucial role, as shown for ZnO@ZIF-71Co-(0.05) [60]. As shown in Fig. 12, introducing ZIF within the semiconductor-metal-based sensor improves the sensitivity and gas response. The maximum response of ZnO@ZIF-71Co-(0.005) for acetone detection was obtained at 250 °C. The coating of ZnO@ZIF-71 with Co atoms showed a significant effect, whereas the sensor with 0.05 g doped with Co metal had 100 times more response than the undoped sensor, as shown in Fig. 12. The Co-doped ZnO@ZIF-71 sensor with acetone had a 50 ppb LOD and a short response-recovery time. In addition, ZnO@ZIF-71Co is a suitable sensor for acetone over ethanol, benzene, and hydrogen; advantageously, the sensor is humidity insensitive. According to the literature, cobalt can catalytically activate the oxygen atoms on ZIF to facilitate gas detection [55].

7.4. The effect of SMOs loading on SMOs@ZIF composite sensor

The effect of SMOs loading on the ZIF for the fabrication of gas sensors affects gas-sensing performance. Fig. 13 shows the impact of In_2O_3 and the mass concentration of ZIF-8 in making a composite to detect NO_2. The investigated mass ratios of In_2O_3/ZIF-8 included 8:1, 4:1, and 2:1. In contrast, the sensor with a 4:1 mass ratio showed the highest NO_2 sensitivity of 16.4, and the sensors with mass ratios of 8:1 and 2:1 had sensitivity of 10.4 and 4.9 %, respectively. Introducing ZIF-8 onto the transition, In_2O_3 NRs reduced the working temperature from 160 °C to 140 °C and all mass ratios' response and recovery times. In_2O_3 NRs during the detection of NO_2 at

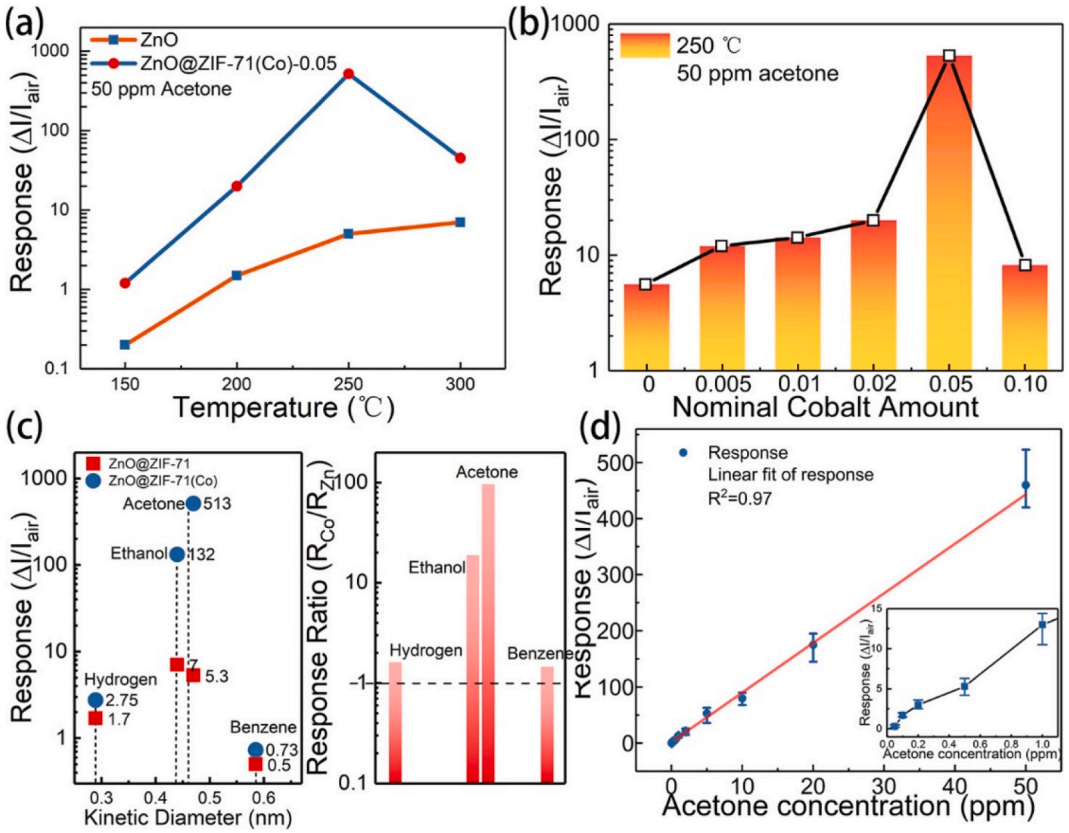

Fig. 12. (a) Investigation of working temperature showing maximum response for acetone at 50 ppm, (b) investigating the gas response from the effect of Co doping at 250 °C, (c) response and sensitivity of ZnO@ZIF-71 and ZnO@ZIF-7(Co) sensor for different analytes at their respective kinetic diameters, and (d) acetone response linearity of ZnO@ZIF-71(Co) sensor [55].

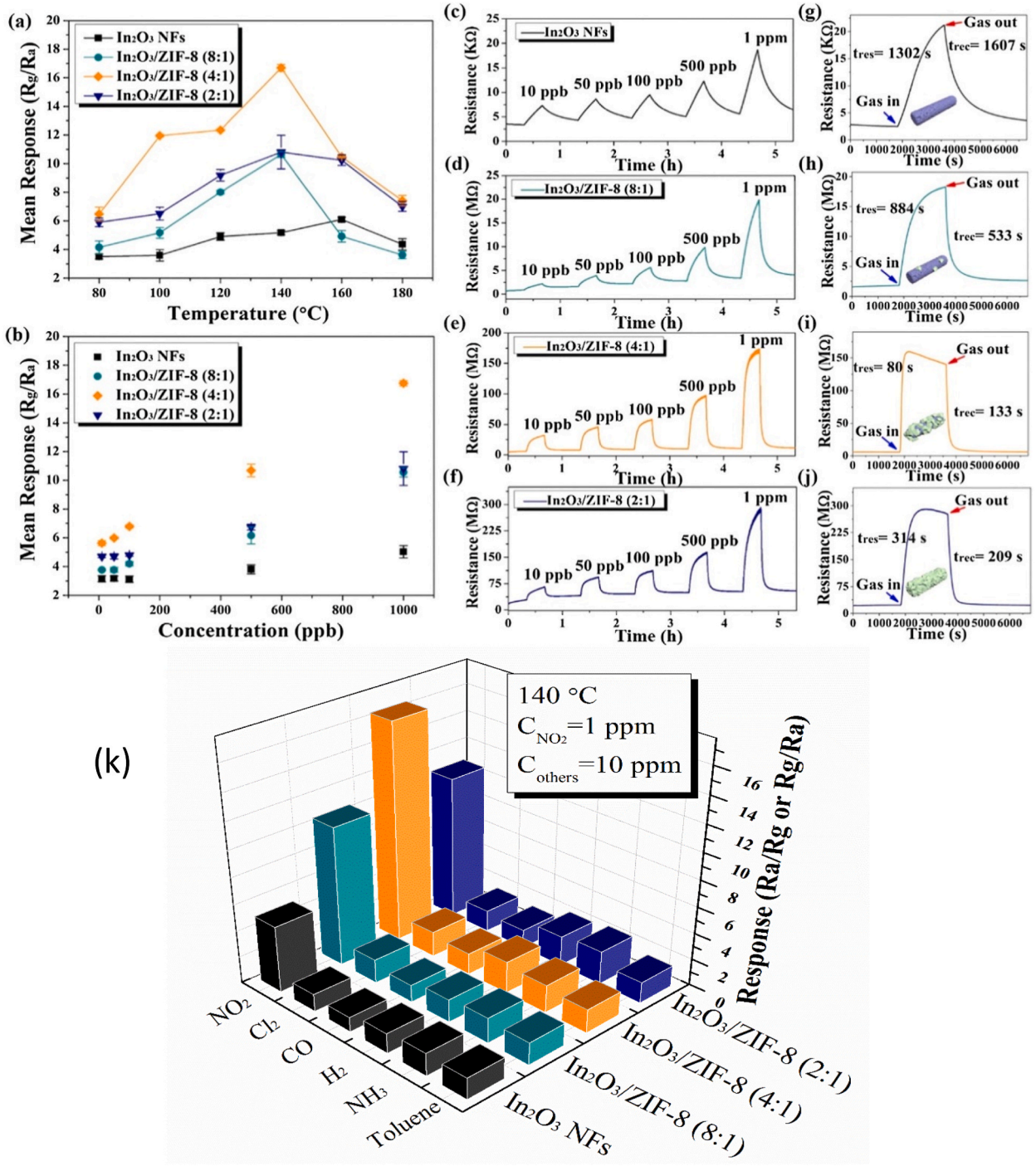

Fig. 13. (a) Working temperature-dependent response curves of In_2O_3 NFs and In_2O_3/ZIF-8 NFs; (b) mean response of NO_2 concentration in the chemiresistive sensor (c–j) response curves of NO_2 at different concentrations on In_2O_3, (d and h) In_2O_3/ZIF-8 (8:1), (e and i) In_2O_3/ZIF-8 (4:1), and (f and j) In_2O_3/ZIF-8 (2:1) sensors at 140 °C, and (k) is the sensitivity graph of the analytes to their respective sensors [57].

its maximum active detecting temperature of 160 °C exhibited a low response, and the sensor failed to reach the plateau as shown in Fig. 13 (c); however, the $In2O_3$/ZIF-8 (4:1) and In_2O_3/ZIF-8 sensors reached plateau stability during the NO_2 detection. The presence of ZIF increases the gas adsorption, as a coating on In_2O_3 has great gas diffusion to facilitate a high gas response. For application purposes, using an In_2O_3/ZIF-8 (4:1) sensor to detect NO_2 is ideal because it can work even at high humidity between 50 and 70 % [57].

Through a literature survey, we tabulated the SMO@ZIF composite to study and understand the effects of ZIFs on SMOs in gas-sensing applications (**Table 1**). It provides an overview of the change in gas sensing performance, including the operational temperature, response-recovery time, and detection limit.

7.5. Advantages and disadvantages of SMOs@ZIF, ZIF-ZIF, and metal-doped SMOs/ZIF sensors

SMOs@ZIF, ZIF-ZIF (also called bi-ZIF), and metal doped-SMO/ZIF composite sensors have shown improved sensing responses as compared to their pristine sensing materials. Improved features include response-recovery time, sensitivity, selectivity, and repeatability. However, all the above mentioned ZIF-based sensors operate at elevated temperatures above 140 °C [54,60,64], which is a significant challenge owing to their higher energy consumption and increases the risk of causing an explosion because some analytes are explosive at elevated temperatures (e.g., propane, butane, and H_2). The sensing materials operating at high temperatures undergo structural changes resulting, in a low lifespan.

7.6. ZIFs-carbon additives composites

ZIFs are reported to have low charge carrier concentrations and high energy bandgaps that arise from their poor gas-responsive character. Usually, ZIFs are integrated with materials such as SMOs [76], doped with transition metals such as cobalt and palladium [55], or other ZIFs [75] to enhance the sensing performance; however, the working temperatures of these sensors are above 140 °C [57]. Recently, carbon-based materials such as reduced graphene oxide (rGO) [61], carbon soot (CNPs) [9], double-walled carbon nanotubes (DWCNT) [62]], and multi-walled carbon nanotubes (MWCNT) [77] have become promising candidates for reducing high working temperature ZIF-based sensors to room working temperature. Working at low temperatures is due to their higher electrical conductivity and higher surface area, which enhance the gas response. However, carbon-based materials exhibit metallic behaviour, making them suffer from selectivity towards the gas of interest compared with semiconductor metal oxides [33, 78]. Utilization of carbon materials reduces the risks of ignition or gas explosions since they can work at room temperature (about 23–26 °C). Moreover, carbon materials alone are unsuitable for gas sensing since they exhibit low response, poor selectivity, and sensitivity. However, carbon additive hybrids improve gas response, response-recovery times, and stability and operate at lower temperatures. The advantage of using a room temperature operating sensor is that the material cannot experience structural changes, which improves the lifespan of gas sensors [79].

In addition to ZIFs properties, such as having the ability for pore size tunability [80], which improves the selectivity of gas analytes based on their kinetic diameters, high adsorption capacity enhances the gas sensitivity response, and the ability to work even in the presence of humidity [46]. These factors make ZIFs exclusive for gas sensing, but they operate at high temperatures. Moreover, introducing carbon-based materials into ZIFs is ideal for chemiresistive gas sensors.

7.6.1. ZIF/MWCNT sensor

According to the work reported by N. Jafari et al., the ZIF-8/MWCNT [77] sensor exhibits eleven times improved sensitivity to formaldehyde compared to the pristine ZIF-8 sensor [37], whereby the operating temperature for the pristine ZIF-8 for the detection of formaldehyde was 300 °C, and while the ZIF/MWCNT works at room temperature. The ZIF-8/MWCNT sensor exhibited excellent repeatability (stability), as shown in Fig. 14 (a). The ZIF-8/MWCNT sensor was susceptible to formaldehyde in water, acetonitrile, ethanol, methanol, and acetone, as shown in Fig. 14 (b), and had a LOD of 5 ppm of formaldehyde.

7.6.2. CNPs/ZnO@ZIF-8 and CNPs@ZIF sensors

The sensor made up of carbon nanoparticles from carbon soot (CNPs), ZnO@ZIF-8, and CNPs/ZnO@ZIF-8 composites detected methanol vapour at room temperature. In this work, ZnO nanorods are coated with ZIF-8 to have ZnO@ZIF-8. ZnO@ZIF-8 is a good proposed sensing material because vapours get filtered by the external ZIF-8 before they can interact with the inner ZnO. Thus, this improves selectivity as the ZIF-8 is designed to have a specific pore diameter that does not allow some vapours to pass through. In addition, as reported, the ZnO@ZIF-8 shows improved sensitivity as compared to gas sensors made up of pristine ZnO and ZIF-8 [37]. ZnO@ZIF-8 sensors did not respond to any of the VOCs (methanol, ethanol, 2-propanol, acetone, chloroform, and ethyl acetate) tested

Table 1
Summarized gas sensing properties of different analytes on SMO@ZIF-composite sensors.

Analyte	Sample	T °C	Response	t/res (s)	t/rec (s)	LOD	Ref
Ethanol	ZnO@ZIF-71	150	13.4	194	442.2	21 ppb	[45]
	ZnO	150	2.57	419	988	207 ppb	[45]
H_2S	WO_3@ZIF-71	250	19.12	118	431	0.67 ppm	[58]
HCHO	WO_3	250	2.24	221	308	4.7 ppm	[58]
NO_2	ZnO@ZIF-8	300	14	16	9	5.6 ppm	[37]
	ZnO	300	18	–	–	–	[37]
	In_2O_3@ZIF-8(4:1)	140	–	80	133	–	[57]
	In_2O_3	140	–	1302	1609	–	[57]

No value (–).

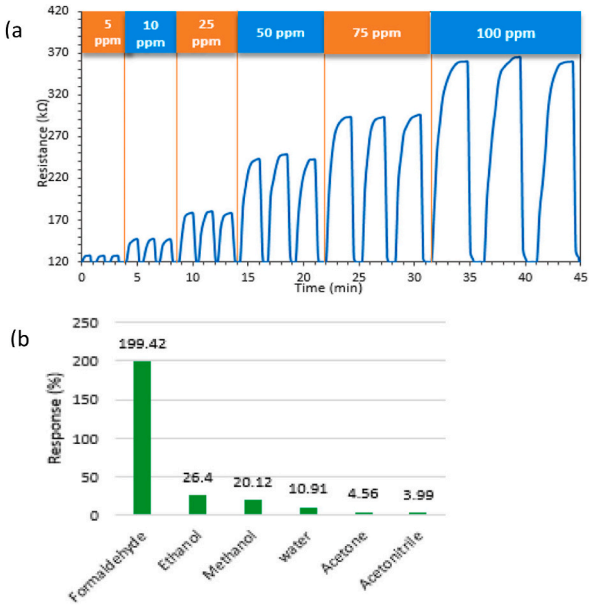

Fig. 14. (b) ZIF-8/MWCNT sensor showing formaldehyde response and repeatability investigation at a concentration from 5 to 100 ppm (b) ZIF-8/MWCNT sensor response to different analytes at 100 ppm [77].

at room temperature, but the pure CNPs sensor responded to VOCs showing little change in responses as the vapour concentration increases (see Fig. 15) [81]. In addition, CNPs/ZnO@ZIF-8 composite showed a 125 times improvement in methanol vapour response compared to the CNPs sensor. However, the extreme changes in methanol response were mainly due to the synergic effect. The CNPs/ZnO@ZIF-8 sensor showed that the gas response is directly proportional to the concentration of methanol and ethanol (see Fig. 15 a-d). The sensor has the quickest response time of 49 s and quickly recovered within 47 s during the detection of methanol vapour. The sensitivity of the gas sensor was optimized by varying the mass amounts of CNPs while the amount of ZnO@ZIF-8 was kept constant (see Fig. 15 e, f, and g). The ZIF-based solid-state gas sensors resist humidity during VOC detection, as experimentally shown in Fig. 15. The dynamic response of CNPs/ZnO@ZIF-8 composite gas sensor at different relative humidities on detecting methanol, i.e., 33 %, 53 %, and 61 %, has shown a response value of 35.4 Ω, 37.8 Ω, and 39.2 Ω, respectively. The gas sensing responses changed slightly, showing a change percentage of about 5 % in relative response from 33 % to 61 % relative humidity, indicating a high resistivity towards water molecules. The response time of the CNP/ZnO@ZIF-8 sensor during the detection of methanol vapour is directly proportional to a change in humidity (see Fig. 15 b) [81].

The carbon soot/ZIF-71 (also written as CNPs/ZIF-71) composite sensor detected acetone vapour at room temperature, and its relative response is directly proportional to the change in acetone concentration, as shown in Fig. 16c. The detection of acetone vapour using a CNPs/ZIF-71 composite sensor was investigated at different humidity conditions, i.e., 28 %, 40 %, and 60 %, showing relative response values of 1.6 Ω, 1.5 Ω, and 1.3 Ω, respectively (Fig. 16 d). It is clearly shown that the relative response of acetone vapour is directly proportional to humidity, although it shows little change in relative response. But it proved that the ZIF-based sensors are hydrophobic, mainly because they are humidity-resistant [9]. Table 2 summarizes the sensing performance of ZIFs. As a single material, ZIF detects vapour analytes at higher temperatures [44,75]. Only a few studies have reported on detecting vapours using a pristine ZIF. They have a slow response time during the detection of gases, as summarized in Table 2. The sensing performances of ZIF-carbon additive sensors are summarized in Table 3.

7.6.3. Low-temperature operation, electronic structure of ZIFs-carbon additives

Nowadays, it is clear that combining carbon materials with semiconductor metal oxides enhances gas sensing performance. Based on their electronic structure, ZIFs are considered to fall under the class of semiconductors because of their wide bandgap. The band gap of ZIF-7, ZIF-8, ZIF-9, and ZIF-67 is 4.8 eV, 5.2 eV, 3.2 eV, and 4.3 eV [84], respectively, while the band gap of carbon materials is more like metals. The band gap of carbon material is very low, the band gap of carbon soot, carbon nanotubes, and graphene is about 0.1 eV [85,86]. It is known that ZIFs are mainly n-type based and carbon materials have the p-type behaviour of semiconductors.

Moreover, ZIF-carbon material hybrids from p-n or heterojunctions with a lower band gap exhibit better gas sensing performances than a single material. The heterojunction is the interface between the ZIF material and the carbon material, wherein the work function decreases, and the composite's conductivity increases compared to pure ZIFs, which leads the sensor to operate at lower temperatures [87,88]. The discussed mechanism needs more experimental work to prove the theory.

The gas sensing performance does not depend only on the electronic structure; other factors that also contribute to sensing are the ability of the material to adsorb gas molecules and morphological variations. Single active layers, carbon-based and ZIF- materials, do not produce satisfying sensing performance; the limitations are that the single components have deficient physical and chemical

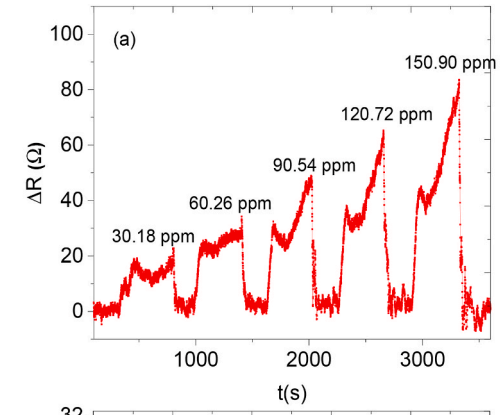

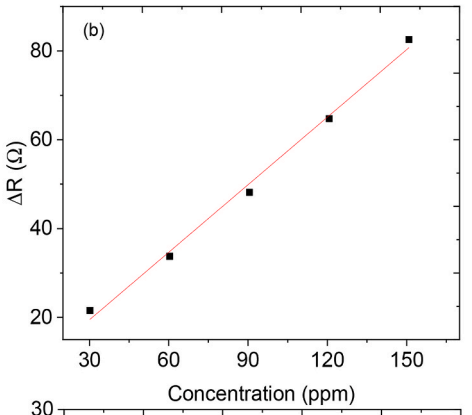

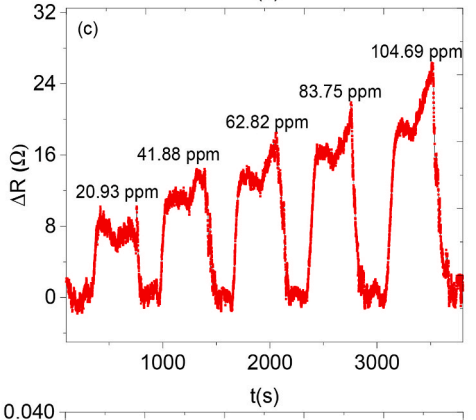

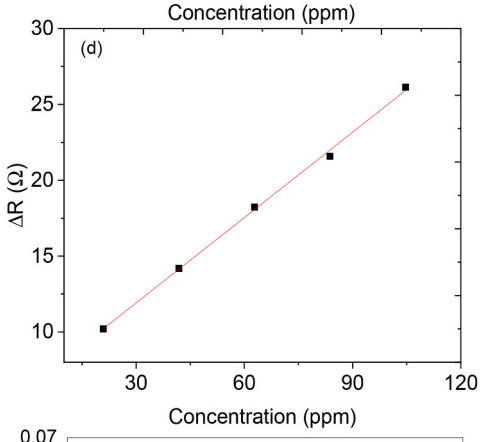

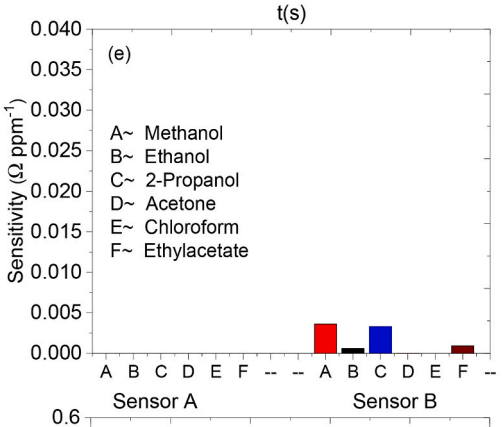

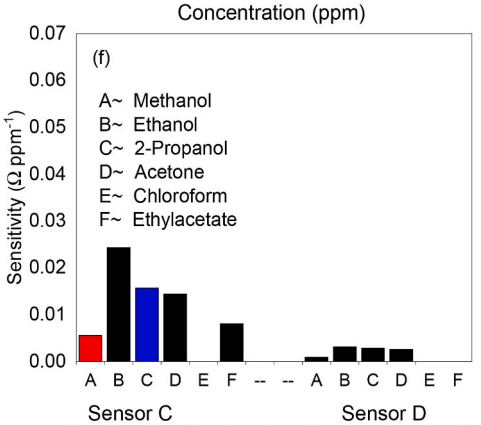

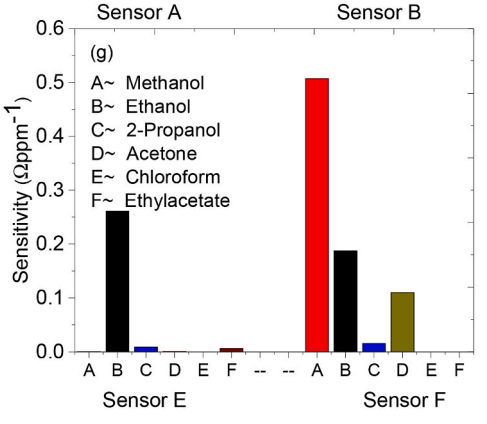

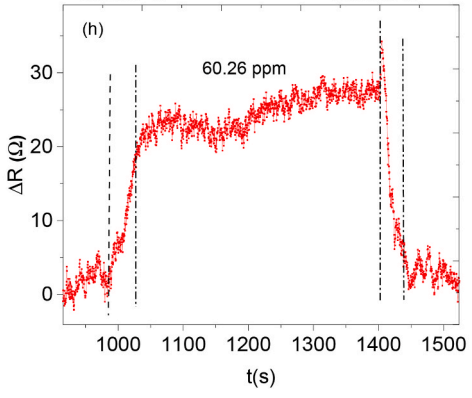

(caption on next page)

Fig. 15. Dynamics response-recovery curve of sensor F (a) and (c) for methanol and ethanol vapour, respectively, and their corresponding calibration curve for methanol and ethanol (b) and (d), respectively. Response-recovery times of methanol on sensor F (d), the sensitivity of the sensors towards various organic vapour (e) for sensors A and B; (f) for sensors C and D; (g) for sensors E and F; (h) the response-recovery profile of sensor F towards methanol [81].

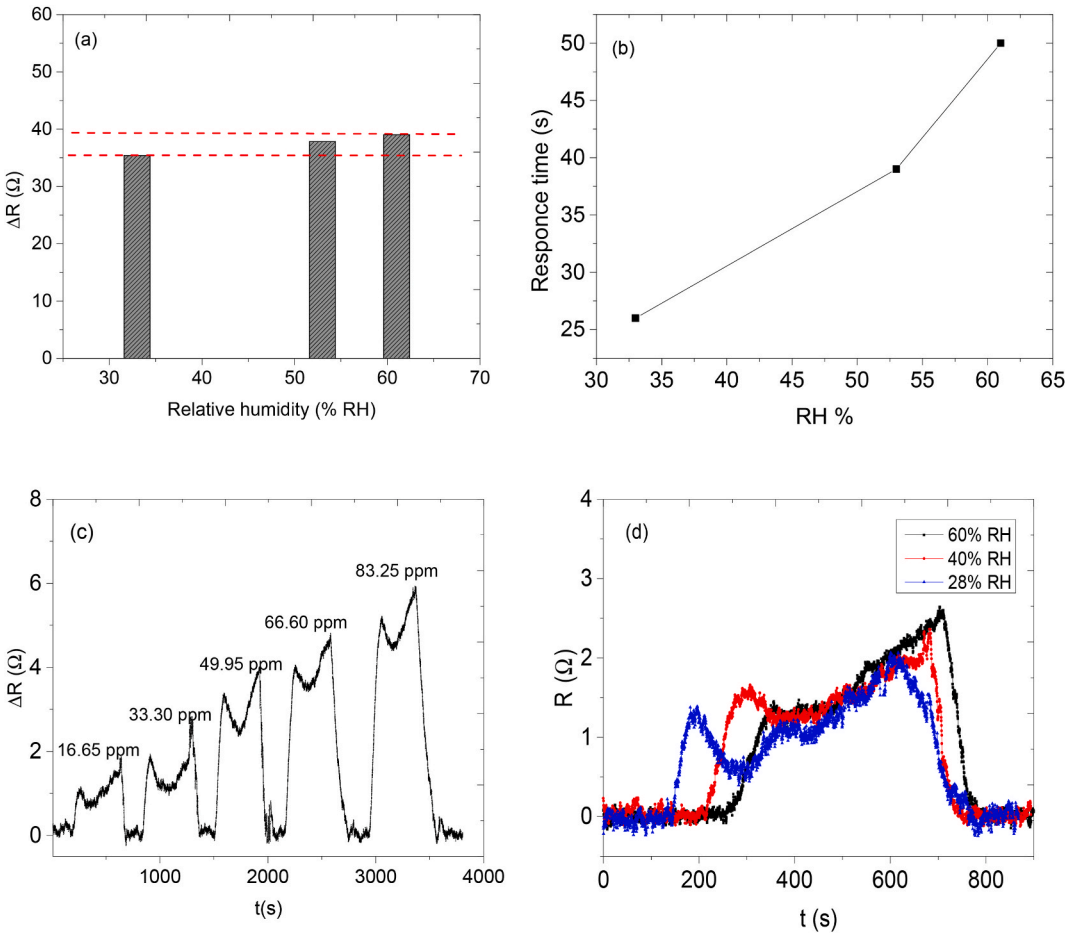

Fig. 16. (a) Humidity bar graph of CNPs/ZnO@ZIF-8 sensor during the detection of acetone vapour, (b) relationship between response time and relative humidity of CNPs/ZnO@ZIF-8 sensor [81], (c) response curve of acetone vapour using CNPs/ZIF-71 sensor and (d) dynamic response of CNPs/ZIF-71 sensor using acetone vapour at different humidity conditions [9].

Table 2
Summarized pristine ZIF sensors and their sensing performances.

Analyte	Sample	Temp °C	Response (Ohms)	t/resp (mins)	t/recov (mins)	Ref
Formaldehyde	ZIF-67	150	13.9 at 100 ppm	–	–	[44]
Toluene	ZIF-67	180	1.1 at 90 ppm	150	–	[75]
Hydrogen	ZIF-8+ZIF-67	180	7.2 at 90 ppm	186	–	[75]
Hydrogen	ZIF-67	180	1.5 at 90 ppm	132	–	[75]

No value (–).

properties. ZIF materials sensors improve selectivity towards the gas of interest and humidity interferences; those sensors cannot operate at room temperature. Carbon materials can operate at room temperature, but the lack of selectivity towards the targeted gas and the fact that they are easily affected by humidity are significant drawbacks; however, the ZIF-carbon material has a hybrid synergetic effect on gas sensing. Room temperature sensors are highly recommended to save energy consumption and increase sensor lifespan [89].

Table 3
Gas sensing properties of ZIF and carbon additives combination operating at room temperature.

Analyte	Sample	Response (Ohms)	t/res (s)	t/rec (s)	LOD	Ref
Acetone	ZIF-8/MWCNT	0.4 at 20 ppm	59	58	1.7 ppb	[82]
Ammonia	ZIF-8/CNT	20 at 100 ppm	120	300	208 ppb	[83]
Ethanol	CNPs/ZnO@ZIF-8	9 at 21 ppm	–	–	–	[81]
Acetone	ZIF-67/carbon soot	2 at 16.7 ppm	53	43	484 ppb	[9]
Ammonia	ZIF-8/rGO	0.9 at 30 ppm	63	52	74 ppb	[77]
Methanol	CNPs/ZnO@ZIF-8	20 at 30 ppm	49	47	60 ppb	[81]

No value(−).

7.6.4. Advantages and challenges of using carbon/SMOs-ZIFs and ZIF-carbon additives hybrids

The presence of carbon material in sensing has received considerable attention in gas-sensing applications because of its ability to work at room temperature [9 [61,62,77]. However, there are some drawbacks to using pristine carbon materials in gas-sensing applications, including poor selectivity, low sensitivity, and high reactivity to polar-based analytes such as ammonia, water, and nitrogen dioxide [59]. Carbon-based sensors are known to have poor reproducibility performance for real-life applications, sensors should have good reproducibility and selectivity [59,76], which is why SMO-carbon and ZIFs-carbon additives grow intensively. Unfortunately, the amounts of carbon materials and ZIFs needed to make a composite that performs very well resulted in no drawback. Having a lot of carbon material in a ZIFs-carbon composite may result in poor selectivity, low sensitivity, responsiveness to humidity, and poor repeatability. Therefore, getting appropriate amounts of carbon and ZIFs as reagents is still under research. In addition, ZIF-carbon sensors should exhibit a higher gas-sensing response than high-operating sensors.

7.7. The future room temperature gas sensors

Most gas sensors, including SMO-based sensors and ZIF-based sensors, operate at high temperatures of approximately 140–400 °C, resulting in high sensitivity and response [90–96]. The fabricated sensors are attached to small heaters to obtain a high working temperature; however, the heaters are costly, and high temperature-based sensors lead to increased power consumption. Thus, there is a need for room-temperature gas sensors; however, these sensors have higher sensing responses than room-temperature (carbon--based) sensors [97]. The major drawback in both high and low-operating temperature sensors is that most of them suffer from selectivity, and carbon-based sensors suffer from humidity as well, which opens the ZIF-carbon material hybrid sensors' field of research because they can work in the presence of moisture and at room temperature. Gas selectivity is possible through ZIF pore size tunability. The ZIF-carbon hybrid sensors are expected to grow rapidly as promising future sensors to assist the system owing to their low working temperature, high surface area, pore size tunability, good absorption capacity, and good electrical conductivity [37,51,57]. All of these excellent properties positively impact the improvement of chemiresistive gas sensors.

Conclusion and future perspectives

This review discusses the growth of ZIF-based gas sensors from high working temperatures to energy-saving sensor devices. We are in the fourth industrial revolution (4IR), rapidly changing the world with advanced artificial intelligence technology. The world is developing suitable materials for gas sensors that can allow devices to work at room temperature and have good sensing performance. Gas devices will not only be installed in buildings and areas where toxic gas can escape but might soon be integrated into our cell phones and tablets. Thus, carbon-ZIF-based composites are promising sensing materials for gas sensing devices because of their ability to work at low temperatures, cheap synthesis, and longer life span. However, these materials need improved properties to enhance their sensitivity and fast recovery response. ZIF with nanorod (SMOs@ZIFs) networks are promising candidates for use in real gas-sensing applications, but other morphologies have room to be explored for sensor performance improvement. Cabon/SMO@ZIFs and ZIF-carbon additive composites exhibit improved sensing performance than their single materials, a synergetic effect occurs when combining the materials. Inexpensive ZIF-based sensors improve the selectivity towards the gas of interest by reducing the pores of the materials and working in the presence of humidity; only a few reports are available on room-temperature ZIF-based gas sensors. Among the various strategies to improve ZIF-based sensors, ZIF-carbon materials were found to be more promising as they operate at room temperature. However, the appropriate amounts of ZIFs and carbon materials are under research to form good heterojunctions that do not possess drawbacks.

Data availability

Data will be made available on request.

CRediT authorship contribution statement

Malepe Lesego: Data curation, Formal analysis, Investigation, Methodology, Writing - original draft. **Derek T. Ndinteh:** Conceptualization, Formal analysis, Methodology, Supervision, Validation, Investigation, Resources, Writing - review & editing.

Patrick Ndungu: Conceptualization, Formal analysis, Funding acquisition, Methodology, Resources, Supervision, Validation, Data curation, Writing - review & editing. **Messai A. Mamo:** Conceptualization, Data curation, Formal analysis, Funding acquisition, Investigation, Project administration, Supervision, Validation, Resources, Visualization, Writing - review & editing.

Declaration of competing interest

The authors declare that they have no known competing financial interests or personal relationships that could have appeared to influence the work reported in this paper.

Acknowledgements

This study was funded by the University of Johannesburg, South Africa.

References

[1] S.E. Bauer, U. Im, K. Mezuman, C.Y. Gao, Desert dust, industrialization, and agricultural fires: health impacts of outdoor air pollution in Africa, J. Geophys. Res. Atmos. 124 (2019) 4104–4120.
[2] R. Baron, J. Saffell, Amperometric gas sensors as a low cost emerging technology platform for air quality monitoring applications: a Review, ACS Sens. 2 (2017) 1553–1566.
[3] Z. Song, Z. Wei, B. Wang, Z. Luo, S. Xu, W. Zheng, H. Yu, M. Li, Z. Huang, J. Zang, F. Yi, H. Liu, Sensitive room-temperature H_2S gas sensors employing SnO_2 quantum wire/reduced graphene oxide nanocomposites, Chem. Mater. 28 (2016) 1205–1212.
[4] X. Liang, T. Zhong, B. Quan, B. Wang, H. Guan, Solid-state potentiometric SO_2 sensor combining NASICON with V_2O_5-doped TiO_2 electrode, Sensors Actuators, B Chem. 134 (2008) 25–30.
[5] H. Im, A.A. Almutairi, S. Kim, M. Sritharan, S. Kim, Y. Yoon, On MoS_2 thin-film transistor design consideration for a NO_2 gas sensor, ACS Sens. 4 (2019) 2930–2936.
[6] A. Hastir, N. Kohli, R. Chand, Ag doped ZnO nanowires as highly sensitive ethanol gas sensor, Mater. Today Proc. 4 (2017) 9476–9480.
[7] B. Wang, X.S. Dong, Z. Wang, Y.F. Wang, Z.Y. Hou, MEMS-based ionization gas sensors for VOCs with array of nanostructured silicon needles,", ACS Sens. 5 (2020) 994–1001.
[8] S. Cao, Z. Huang, D. Yang, G. Zhang, Improving gas-sensing performance based on MOS nanomaterials: a review, Materials 14 (2021) 4263.
[9] L. Malepe, T.D. Ndinteh, P. Ndungu, M.A. Mamo, A humidity-resistant and room temperature carbon soot@ZIF-67 composite sensor for acetone vapour detection, Nanoscale Adv. 5 (2023) 1956–1969.
[10] S. Sohrabi, Ghasemzadeh, Z. Ghoreishi, M.R. Majidi, Y. Yoon, N. Dizge, A. Khataee, Metal-organic frameworks (MOF)-based sensors for detection of toxic gases: a review of current status and future prospects, Mater. Chem. Phys. 299 (2023), 127512.
[11] M.K. Smith, D.G. Martin-Peralta, P.A. Pivak, K.A. Mirica, Fabrication of solid-state gas sensors by drawing: an undergraduate and high school introduction to functional nanomaterials and chemical detection, J. Chem. Educ. 94 (2017) 1933–1938.
[12] S. Li, D. Liu, N. Tian, Y. Liang, C. Gao, S. Wang, Y. Zhang, High-performance temperature sensor based on silver nanowires, Mater. Today Commun. 20 (2019), 100546.
[13] D.W. Hwang, S. Lee, M. Seo, T.D. Chung, Recent advances in electrochemical non-enzymatic glucose sensors – a review, Anal. Chim. Acta 1033 (2018) 1–34.
[14] J.A.R. Ruiz, S. Vallejos, F.C. Garcia, J.M. Garcia, Polymer-based chemical sensors, Chemosensors 6 (2018) 42.
[15] A.C. Power, B. Gorey, S. Chandra, J. Chapman, Carbon nanomaterials and their application to electrochemical sensors : a review, Nanotechnol. Rev. 7 (2018) 19–41.
[16] M.S. Yao, W.H. Li, G. Xu, Metal–organic frameworks and their derivatives for electrically-transduced gas sensors, Coord. Chem. Rev. 426 (2021), 213479.
[17] J. Huang, Q. Wan, Gas sensors based on semiconducting metal oxide one-dimensional nanostructures, Sensors 9 (2009) 9903–9924.
[18] L. Malepe, D. Ndinteh, M.A. Mamo, The effect of measurement parameters on the performance of the sensors in the detection of organic compound vapours, Chem. Phys. Impact 4 (2021), 100068.
[19] A. Liu, Y. Meng, H. Zhu, Y.-Y. Noh, G. Liu, F. Shan, Electrospun p -type nickel oxide semiconducting nanowires for low-voltage field-effect transistors, ACS Appl. Mater. Interfaces 10 (2018) 25841–25849.
[20] R. Alrammouz, J. Podlecki, P. Abboud, B. Sorli, R. Habchi, A review on flexible gas sensors: from materials to devices, Sensors Actuators, A Phys. 284 (2018) 209–231.
[21] A. Dey, Semiconductor metal oxide gas sensors: a review, Mater. Sci. Eng. B: Solid-State Materials for Advanced Technology 229 (2018) 206–217.
[22] Y. Seekaew, A. Wisitsoraat, D. Phokharatkul, C. Wongchoosuk, Room temperature toluene gas sensor based on TiO_2 nanoparticles decorated 3D graphene-carbon nanotube nanostructures, Sensors Actuators, B Chem. 279 (2019) 69–78.
[23] T.P. Mokoena, H.C. Swart, D.E. Motaung, A review on recent progress of p-type nickel oxide based gas sensors: future perspectives, J. Alloys Compd. 805 (2019) 267–294.
[24] X. Jin, Y. Li, Y. Zheng, Z. Fan, X. Han, W. Wang, T. Lin, Z. Zhu, Nanomaterial design for efficient solar-driven steam generation, ACS Appl. Energy Mater. 2 (2019) 6112–6126.
[25] S.K. Kwak, S. Lee, Polysulfide-breathing/dual-conductive, heterolayered battery separator membranes based on 0D/1D mingled nanomaterial composite mats, Nano Lett. 17 (2017) 2220–2228.
[26] K.S. Kumar, N. Choudhary, Y. Jung, J. Thomas, Recent advances in two-dimensional nanomaterials for supercapacitor electrode applications, ACS Energy Lett. 3 (2018) 482–495.
[27] F. Li, L. Chen, G.P. Knowles, R. Macfarlane, J. Zhang, Hierarchical mesoporous SnO_2 nanosheets on carbon cloth : a robust and flexible electrocatalyst for CO_2 reduction with high efficiency and selectivity, Angew. Chem. 129 (2016) 505–509.
[28] S. Wang, F. Jia, X. Wang, L. Hu, Y. Su, G. Yin, T. Zhou, Z. Feng, P. Kumar, B. Liu, Fabrication of ZnO nanoparticles modi fi ed by uniformly dispersed Ag nanoparticles : enhancement of gas sensing performance, ACS Omega 5 (2020) 5209–5218.
[29] Y.M. Sabri, A.E. Kandjani, S.S.A.A.H. Rashid, C.J. Harrison, S.J. Ippolito, S.K. Bhargava, Soot template TiO_2 fractals as a photoactive gas sensor for acetone detection, Sensors Actuators, B Chem. 275 (2018) 215–222.
[30] A. Nikfarjam, S. Hosseini, N. Salehifar, Fabrication of a highly sensitive single aligned TiO_2 and gold nanoparticle embedded TiO_2 nano-fiber gas sensor, ACS Appl. Mater. Interfaces 9 (2017) 15662–15671.
[31] L. Malepe, P. Ndungu, D.T. Ndinteh, M.A. Mamo, Nickel oxide-carbon soot-cellulose acetate nanocomposite for the detection of mesitylene vapour: investigating the sensing mechanism using an LCR meter coupled to an FTIR spectrometer, Nanomaterials 12 (2022) 727.
[32] A.M. Soleimanpour, S.V. Khare, A.H. Jayatissa, Enhancement of hydrogen gas sensing of nanocrystalline nickel oxide by pulsed-laser irradiation, ACS Appl. Mater. Interfaces 4 (2012) 4651–4657.
[33] V.O. Okechukwu, V. Mavumengwana, I.A. Hümmelgen, M.A. Mamo, Concomitant in Situ FTIR and impedance measurements to address the 2-methylcyclo-pentanone vapor-sensing mechanism in MnO_2 -polymer nanocomposites, ACS Omega 4 (2019) 8324–8333.
[34] J. Xiao, P. Liu, Y. Liang, H.B. Li, G.W. Yang, High aspect ratio β-MnO_2 nanowires and sensor performance for explosive gases, J. Appl. Phys. 114 (2013), 073513.

[35] C. Liu, S.T. Navale, Z.B. Yang, M. Galluzzi, V.B. Patil, P.I. Cao, R.S. Mane, F.J. Stadler, Ethanol gas sensing properties of hydrothermally grown α-MnO_2 nanorods, J. Alloys Compd. 727 (2017) 362–369.

[36] K. Vijayalakshmi, A. Monamary, Highly sensitive H_2O_2 sensor based on annealed MnO_2/Al_2O_3 nanofibers prepared by a novel spray pyrolysis deposition, J. Anal. Appl. Pyrolysis 128 (2017) 268–274.

[37] H. Tian, H. Fan, M. Li, Zeolitic imidazolate framework coated ZnO nanorods as molecular sieving to improve selectivity of formaldehyde gas sensor, ACS Sens. 1 (2016) 243–250.

[38] D. Zhang, Q. Xiang, Simple and efficient size-controllable engineering of zeolitic imidazolate framework (ZIF-8) and M-ZIF-8 by changing addition order, Mater. Lett. 289 (2021), 129418.

[39] M. Weber, J. Kim, J. Lee, J. Kim, I. Iatsunskyi, E. Coy, M. Drobek, A. Julbe, M. Bechelany, S.S. Kim, High-performance nanowire hydrogen sensors by exploiting the synergistic e ff ect of pd nanoparticles and metal-organic framework membranes, ACS Appl. Mater. Interfaces 10 (2018) 34765–34773.

[40] Y. Li, F. Liang, H. Bux, W. Yang, J. Caro, Zeolitic imidazolate framework ZIF-7 based molecular sieve membrane for hydrogen separation, J. Memb. Sci. 354 (2010) 48–54.

[41] Y. Huang, D. Liu, Z. Liu, C. Zhong, Synthesis of zeolitic imidazolate framework membrane using temperature-switching synthesis strategy for gas separation, Ind. Eng. Chem. Res. 55 (2016) 7164–7170.

[42] K.D. Modibane, N.J. Waleng, K.E. Ramohlola, T.C. Maponya, G.R. Monama, K. Makgopa, M.J. Hato, Poly(3-aminobenzoic acid) decorated with cobalt zeolitic benzimidazolate framework for electrochemical production of clean hydrogen, Polymers 12 (2020) 1–14.

[43] A. Malik, M. Nath, Ultrafast catalytic reduction of toxic nitroaromatics and organic colouring dyes by using Au/ZIF-11: efficient wastewater treatment, J. Water Process Eng. 44 (2021), 102362.

[44] E. Chen, H. Yang, J. Zhang, Zeolitic imidazolate framework as formaldehyde gas sensor, Inorg. Chem. 53 (2014) 5411–5413.

[45] B. Chen, Z. Yang, Y. Zhu, Y. Xia, Zeolitic imidazolate framework materials: recent progress in synthesis and applications, J. Mater. Chem. A. 2 (2014) 16811, 1683.

[46] T. Zhou, Y. Sang, Y. Sun, C. Wu, X. Wang, X. Tang, T. Zhang, H. Wang, C. Xie, D. Zeng, Gas adsorption at metal sites for enhancing gas sensing performance of ZnO@ZIF-71 nanorod arrays, Langmuir 35 (2019) 3248–3255.

[47] X. Wu, S. Xiong, Z. Mao, S. Hu, X. Long, A Designed ZnO@ZIF-8 Core–shell nanorod film as a gas sensor with excellent selectivity for H_2 over CO, Chem. Eur J. 23 (2017) 7969–7975.

[48] M. Jian, B. Liu, R. Liu, J. Qu, H. Wang, X. Zhang, Water-based synthesis of zeolitic imidazolate framework-8 with high morphology level at room temperature, RSC Adv. 5 (2015) 48433–48441.

[49] K.S. Park, Z. Ni, A.P. Cote, J.Y. Choi, R. Huang, F.J. Uribe-Romo, H.K. Chae, M. O'keeffe, O.M. Yaghi, Exceptional chemical and thermal stability of zeolitic imidazolate frameworks, Proc. Natl. Acad. Sci. USA 103 (2006) 10186–10191.

[50] M. Yahia, O.H.P. Le, N. Ismail, M. Eshalhi, O. Sundman, A. Rahimpour, M.M. Dal-Cin, N. Tavajohi, Effect of incorporating different ZIF-8 crystal sizes in the polymer of intrinsic microporosity, PIM-1, for CO_2/CH_4 separation, Microporous Mesoporous Mater. 312 (2021), 110761.

[51] J. Zakzeski, A. Dbczak, P.C.A. Bruijnincx, B.M. Weckhuysen, Catalytic oxidation of aromatic oxygenates by the heterogeneous catalyst Co-ZIF-9, Appl. Catal. Gen. 394 (2011) 79–85.

[52] W. Xia, J. Zhu, W. Guo, L. An, D. Xia, R. Zou, Well-defined carbon polyhedrons prepared from nano metal-organic frameworks for oxygen reduction, J. Mater. Chem. A 2 (2014) 11606–11613.

[53] M. Tu, C. Wiktor, C. Rosler, R.A. Fischer, Rapid room temperature syntheses of zeolitic-imidazolate framework (ZIF) nanocrystals, Chem. Commun. 50 (2014) 13258–13260.

[54] M.S. Yao, W.X. Tang, G.E. Wang, B. Nath, G. Xu, MOF thin film-coated metal oxide nanowire array: significantly improved chemiresistor sensor performance, Adv. Mater. 28 (2016) 5229–5234.

[55] C. Xie, D. Zeng, T. Zhou, S. Chen, X. Wang, Catalytic activation of cobalt doping sites in ZIF-71-coated ZnO nanorod arrays for enhancing gas-sensing performance to acetone, ACS Appl. Mater. Interfaces 12 (2020) 48948–48956.

[56] D. Zhu, Y. Huang, J. ji Cao, S.C. Lee, M. Chen, Z. Shen, Cobalt nanoparticles encapsulated in porous nitrogen-doped carbon: oxygen activation and efficient catalytic removal of formaldehyde at room temperature, Appl. Catal. B Environ. 258 (2019), 117981.

[57] Y. Liu, R. Wang, T. Zhang, S. Liu, T. Fei, Zeolitic imidazolate framework-8 (ZIF-8)-coated In_2O_3 nanofibers as an efficient sensing material for ppb-level NO_2 detection, J. Colloid Interface Sci. 541 (2019) 249–257.

[58] Y. Zhou, T. Zhou, Y. Zhang, L. Tang, Q. Guo, M. Wang, Synthesis of core-shell flower-like WO_3@ZIF-71 with enhanced response and selectivity to H_2S gas, Solid State Ionics 350 (2020), 115278.

[59] W. Koo, H. Cho, D. Kim, Y.H. Kim, H. Shin, R. M Penner, I. Kim, Chemiresistive hydrogen sensors: fundamentals, recent advances, and challenges, ACS Nano 14 (2020) 14284–14322, 2020.

[60] H. Kim, W. Kim, S. Cho, J. Park, G.Y. Jung, Molecular sieve based on a pmma/zif-8 bilayer for a co-tolerable H_2 sensor with superior sensing performance, ACS Appl. Mater. Interfaces 12 (2020) 28616–28623.

[61] N. Garg, M. Kumar, N. Kumari, A. Deep, A.L. Sharma, Chemoresistive room-temperature sensing of ammonia using zeolite imidazole framework and reduced graphene oxide (ZIF-67/RGO) composite, ACS Omega 5 (2020) 27492–27501.

[62] G. Chimowa, L. Yang, P. Lonchambon, T. Hungría, L. Datas, C. Vieu, Flahaut, Tailoring of DWNTs for formaldehyde sensing through encapsulation of selected materials, Phys. Status Solidi 216 (2019).

[63] M. Drobek, J.H. Kim, M. Bechelany, C. Vallicari, A. Julbe, S.S. Kim, MOF-based membrane encapsulated ZnO nanowires for enhanced gas sensor selectivity, ACS Appl. Mater. Interfaces 8 (2016) 8323–8328.

[64] A.A. Tezerjania, R. Halladj, S. Askari, Different view of solvent effect on the synthesis methods of zeolitic imidazolate framework-8 to tuning the crystal structure and properties, RSC Adv. 11 (2021) 19914–19923.

[65] M. Tu, C. Wiktor, C. Rosler, R.A. Fischer, Rapid room temperature syntheses of zeolitic-imidazolate framework (ZIF) nanocrystals, Chem. Commun. 50 (2014) 13258–13260.

[66] M. Shahsavari, P.M. Jahani, I. Sheikhshoaie, S. Tajik, A.A. Afshar, M.B. Askari, P. Salarizadeh, A. Di Bartolomeo, H. Beitollahi, Green synthesis of zeolitic imidazolate frameworks: a review of their characterization and industrial and medical applications, Materials 15 (2022) 447.

[67] J. Liu, C. Liu, A. Huang, Co-based zeolitic imidazolate framework ZIF-9 membranes prepared on α-Al2O3 tubes through covalent modification for hydrogen separation, Int. J. Hydrogen Energy 45 (2020) 703–711.

[68] Y. Li, L.H. Wee, J.A. Martens, I.F.J. Vankelecom, ZIF-71 as a potential filler to prepare pervaporation membranes for bio-alcohol recovery, J. Mater. Chem. A 2 (2014) 10034–10040.

[69] X. Wang, J. Zhou, H. Fu, W. Li, X. Fan, G. Xin, J. Zheng, X. Li, MOF derived catalysts for electrochemical oxygen reduction, J. Mater. Chem. A 2 (2014) 14064–14070.

[70] K. S. Park, Z. Ni, A. P. Côté, J. Y. Choi, R. Huang, F. J. Uribe-Romo, H. K. Chae, M. O'Keeffe, and O. M. Yaghi, Exceptional chemical and thermal stability of zeolitic imidazolate frameworks, Proc. Natl. Acad. Sci. USA,103 (27) 10186–10191.

[71] C. Duan, Y. Yu, H. Hu, Recent progress on synthesis of ZIF-67-based materials and their application to heterogeneous catalysis, Green Energy Environ. 7 (2022) 3–15.

[72] T. Zhou, Y. Sanga, X. Wanga, C. Wua, D. Zenga, C. Xie, Pore size dependent gas-sensing selectivity based on ZnO@ZIF nanorod arrays, Sensor. Actuator. B 258 (2018) 1099–1106.

[73] T. Zhou, Y. Sanga, X. Wanga, C. Wua, D. Zenga, C. Xie, Pore size dependent gas-sensing selectivity based on ZnO@ZIF nanorod arrays, Sensor. Actuator. B 258 (2018) 1099–1106.

[74] S.M. Majhi, S.T. Navale, A. Mirzaei, H. Woo Kim, S.S. Kim, Strategies to boost chemiresistive sensing performance of In_2O_3-based gas sensors: an overview, Inorg. Chem. Front. 10 (2023) 3428–3467.

[75] D. Matatagui, A. Sainz-Vidal, I. Gràcia, E. Figueras, C. Cané, J.M. Saniger, Chemoresistive gas sensor based on ZIF-8/ZIF-67 nanocrystals, Sensors Actuators, B Chem. 274 (2018) 601–608.
[76] D. Zhu, Y. Huang, J. Cao, S. Cheng, M. Chen, Z. Shen, Environmental Cobalt nanoparticles encapsulated in porous nitrogen-doped carbon : oxygen activation and effi cient catalytic removal of formaldehyde at room temperature, Appl. Catal. B Environ. 258 (2019), 117981.
[77] N. Jafari, S. Zeinali, Highly rapid and sensitive formaldehyde detection at room temperature using a ZIF-8/mwcnt nanocomposite, ACS Omega 5 (2020) 4395–4402.
[78] P.R. Chung, C.T. Tzeng, M.T. Ke, C.Y. Lee, Formaldehyde gas sensors: a review, Sensors 13 (2013) 4468–4484.
[79] G.E. Olifant, V. Mavumengwana, I.A. Hümmelgen, M.A. Mamo, Understanding the sensing mechanism of carbon nanoparticles: MnO_2 –PVP composites sensors using in situ FTIR—online LCR meter in the detection of ethanol and methanol vapor, J. Mater. Sci. Mater. Electron. 30 (2019) 3552–3562.
[80] I.S. Amiinu, X. Liu, Z. Pu, W. Li, Q. Li, J. Zhang, H. Tang, H. Zhang, S. Mu, From 3D ZIF nanocrystals to Co-n_x/C nanorod array electrocatalysts for ORR, OER, and Zn-air batteries, Adv. Funct. Mater. 28 (2018), 1704638.
[81] L. Malepe, D.T. Ndinteh, P. Ndungu, M.A. Mamo, Selective detection of methanol vapour from a multicomponent gas mixture using a CNPs/ZnO@ZIF-8 based room temperature solid-state sensor, RSC Adv. 12 (2022), 27094.
[82] S. Homayoonnia, S. Kim, ZIF-8/MWCNT-nanocomposite based-resistive sensor for highly selective detection of acetone in parts-per-billion: potential noninvasive diagnosis of diabetes, Sens. Actuators, A 393 (2023), 134197.
[83] W. Yan, S. Zhou, M. Ling, X.S. Peng, H. Zhou, NH_3 sensor based on ZIF-8/CNT operating at room temperature with immunity to humidity, Inorganics 10 (2022) 193.
[84] K.T. Butler, C.H. Hendon, A. Walsh, Designing porous electronic thin-film devices: band offsets and heteroepitaxy, Faraday Discuss 201 (2017) 207–219.
[85] C. Russo, B. Apicella, A. Tregrossi, A. Ciajolo, K.C. Le, S. Torok, P. Bengtsson, Optical band gap analysis of soot and organic carbon in premixed ethylene flames: comparison of in-situ and ex-situ absorption measurements, Carbon 158 (2020) 89–96.
[86] M. Ouyang, J. Huang, C.L. Cheung, C.M. Lieber, Energy gaps in "metallic" single-walled carbon nanotubes, Science 292 (2001) 702–705.
[87] S.M. Majhi, abd Ali Mirzaei, S. Navale, H.W. Kim, S.S. Kim, Boosting the sensing properties of resistive-based gas sensors by irradiation techniques: a review, Nanoscale 13 (2021) 4728–4757.
[88] V.M. Aroutiounian, Metal oxide gas sensors decorated with carbon nanotubes, Lith. J. Phys. 55 (2015) 319–329.
[89] S.M. Majhi, Mirzaei Ali, H.W. Kim, S.S. Kim, T.W. Kim, Recent advances in energy-saving chemiresistive gas sensors: a review, Nano Energy 79 (2021), 105369.
[90] A. Sarkar, S. Maity, P. Chakraborty, S.K. Chakraborty, Synthesize of ZnO Nano structure for toxic gas sensing application, Procedia - Procedia Comput. Sci. 92 (2016) 199–206.
[91] R. Ab Kadir, Z. Li, A.Z. Sadek, R.A. Rani, A.S. Zoolfakar, M.R. Field, J.Z. Ou, A.F. Chrimes, K. Kalantar-Zadeh, Electrospun granular hollow SnO2 nanofibers hydrogen gas sensors operating at low temperatures, J. Phys. Chem. C 118 (2014) 3129–3139.
[92] H.D. Chen, K.L. Jin, J.C. Xu, J.B. Han, H.X. Jin, D.F. Jin, X.L. Peng, B. Hong, J. Li, Y.T. Yang, J. Gong, H.L. Ge, X.Q. Wang, High-valence cations-doped mesoporous nickel oxides nanowires: nanocasting synthesis, microstructures and improved gas-sensing performance, Sensors Actuators, B Chem. 296 (2019), 126622.
[93] B. Han, X. Liu, X. Xing, N. Chen, X. Xiao, S. Liu, Y. Wang, A high response butanol gas sensor based on ZnO hollow spheres, Sensors Actuators B. Chem. 237 (2016) 423–430.
[94] Y. Li, D. Deng, X. Xing, N. Chen, X. Liu, X. Xiao, Y. Wang, A high performance methanol gas sensor based on palladium-platinum-In2O3 composited nanocrystalline SnO_2, Sensors Actuators B. Chem. 237 (2016) 133–141.
[95] P.P. Sahay, R.K. Nath, Al-doped ZnO thin films as methanol sensors, Sensors Actuators B. Chem. 134 (2008) 654–659.
[96] A. Hastir, N. Kohli, R.C. Singh, Ag doped ZnO nanowires as highly sensitive ethanol gas sensor, Mater. Today Proc. 4 (2017) 9476–9480.
[97] E. Cao, H. Wang, X. Wang, Y. Yang, W. Hao, L. Sun, Y. Zhang, Enhanced ethanol sensing performance for chlorine doped nanocrystalline $LaFeO_3$-δ powders by citric sol-gel method, Sensors Actuators, B Chem. 251 (2017) 885–893.